

Perturbativity in the presence of ultraslow-roll dynamics

Gabriele Franciolini^{1,2,*} Antonio Junior Iovino^{1,2,†} Marco Taoso^{3,‡} and Alfredo Urbano^{1,2,§}

¹*Dipartimento di Fisica, Sapienza Università di Roma, Piazzale Aldo Moro 5, 00185, Roma, Italy*

²*INFN, Sezione di Roma, Piazzale Aldo Moro 2, 00185, Roma, Italy*

³*Istituto Nazionale di Fisica Nucleare, Sezione di Torino, via P. Giuria 1, I-10125 Torino, Italy*



(Received 10 July 2023; accepted 4 June 2024; published 28 June 2024)

We discuss the issue of perturbativity in single-field inflationary models with a phase of ultraslow-roll (USR) tailor suited to generate an order-one abundance of primordial black holes (PBHs). More in detail, we impose the condition that loop corrections made up of short-wavelength modes enhanced by the USR dynamics do not alter the tree-level power spectrum of curvature perturbations. In our analysis, the USR phase is preceded and followed by two stages of ordinary slow-roll (SR), and we model the resulting SR/USR/SR dynamics using both instantaneous and smooth transitions. Focusing on scales relevant for cosmic microwave background observations, we find that it is not possible, with these arguments, to rule out the scenario of PBH formation via USR, not even in the limit of instantaneous transition. However, we also find that loop corrections of short modes on the power spectrum of long modes, even though not large enough to violate perturbativity requirements, remain appreciable and, most importantly, are not tamed in realistic realizations of smooth SR/USR/SR transitions. This makes perturbativity a powerful theoretical tool to constrain USR dynamics. We extend the analysis at any scale beyond those relevant for cosmic microwave background observations. We find that loop corrections of short modes remain within the few percent if compared to the tree-level power spectrum. However, we also find one notable exception of phenomenological relevance: we show that the so-called dip in the power spectrum of curvature perturbation is significantly reduced beyond the tree-level computation.

DOI: [10.1103/PhysRevD.109.123550](https://doi.org/10.1103/PhysRevD.109.123550)

I. INTRODUCTION

In this work, we consider the so-called standard scenario of primordial black hole (PBH) formation [1–3]. In this scenario, the formation of PBHs during the early Universe is an exceptional phenomenon in which extremely dense regions of radiation energy are tightly packed to the point of gravitational collapse [4–6]. General relativity and the inflationary stage preceding the radiation epoch offer a mechanism to generate such overdensities: small-scale curvature perturbations, stretched way beyond the horizon by the inflationary expansion, are transferred to the radiation fluid after the end of inflation at around the time of their horizon reentry. In order to truly trigger a gravitational collapse of the radiation fluid, the amplitude of such small-scale curvature perturbations needs to be greatly enhanced by some dynamics during the inflationary stage. This statement can be made more quantitative by introducing the dimensionless power spectrum $\mathcal{P}(k)$ which gives the contribution to the variance of the curvature perturbation field per bin of $\log k$, with k the comoving

wave number in Fourier space. At scales relevant for cosmic microwave background (CMB) observations (that is, $0.005 \lesssim k[\text{Mpc}^{-1}] \lesssim 0.2$) we typically have $\mathcal{P}(k) = O(10^{-9})$; at smaller scales ($1.5 \times 10^{13} \lesssim k[\text{Mpc}^{-1}] \lesssim 1.5 \times 10^{14}$) asteroid-mass PBHs may comprise the totality of dark matter (DM) observed in the Universe but their formation requires $\mathcal{P}(k) = O(10^{-2})$ (for recent reviews see [7–11]). Theory side, therefore, what makes the formation of PBHs an exceptional phenomenon is the fact that it requires a seven-order-of-magnitude enhancement of the small-scale power spectrum with respect to the value observed at large scales.

In the context of single-field models of inflation, the above-mentioned enhancement can be dynamically realized by introducing a phase of ultraslow-roll (USR) [12–34] during which the inflaton field, after the first conventional phase of slow-roll (SR) that is needed to fit large-scale cosmological observations, almost stops the descent along its potential (typically because of the presence of a quasi-stationary inflection point) before starting rolling down again in a final stage of SR dynamics that eventually ends inflation. In this work, we shall refer to this three-stage dynamics as SR/USR/SR.

A very legitimate question is whether the USR dynamics is consistent with perturbativity. Technically speaking, the

*gabriele.franciolini@uniroma1.it

†antoniojunior.iovino@uniroma1.it

‡marco.taoso@to.infn.it

§alfredo.urbano@uniroma1.it

dimensionless power spectrum of curvature perturbation $\mathcal{P}(k)$ is typically computed within the free theory. However, curvature perturbations, being gravitational in nature, feature an intricate architecture of nonlinear interactions. The effect of nonlinear interactions is twofold. On the one hand, they generate, in addition to the variance, nonzero higher-order cumulants that may leave a peculiar non-Gaussian pattern to the statistics of the curvature field. On the other hand, the variance itself gets corrected with respect to the value computed within the free theory. In this paper, we focus on the second effect and, on very general grounds, we define the perturbative criterion

$$\mathcal{P}(k) \equiv \mathcal{P}_{\text{tree}}(k)[1 + \Delta\mathcal{P}_{\text{1-loop}}(k)] \Rightarrow \Delta\mathcal{P}_{\text{1-loop}}(k) \stackrel{!}{<} 1, \quad (1)$$

meaning that the power spectrum computed within the free theory (the “tree-level” power spectrum in the above equation) must be larger than the corrections $\Delta\mathcal{P}$ introduced by the presence of interactions. Such corrections can be organized in a formal series expansion, and we will focus in particular on the first-order term, dubbed “1-loop” in the above equation.

The gut feeling is that, unless one is led to consider $\mathcal{P}_{\text{tree}}(k) = O(1)$, perturbativity should be under control. However, Ref. [35] made the bold claim that, in the presence of USR, the perturbativity condition in Eq. (1) could be violated at scales k relevant for CMB observations; even more strikingly, Ref. [35] argues that USR dynamics tailored to generate a sizable abundance of asteroid- or solar-mass PBHs are ruled out. What makes the claim of Ref. [35] so hard to accept is that it basically says that loop of short modes alters the correlation of long CMB modes. This is counterintuitive since it clashes with the intuition that physics at different scales should be decoupled.

Given the above, it is not surprising that Ref. [35] sparked an intense debate mostly exclusively polarized on defending or disproving the claim that PBH formation from single-field inflation is ruled out [36–44]. In this paper, we bury the hatchet and critically examine the consequences of Eq. (1) in the presence of single-field inflation with USR dynamics.

Our analysis is structured as follows. In Sec. II, we set the ground for the one-loop computation; in particular, we define all our conventions in Sec. II A, the SR/USR/SR background dynamics in Sec. II B and the interaction Hamiltonian in Sec. II C. In Sec. III, we compute the one-loop correction to the curvature power spectrum within the setup described in Sec. II A; in particular, in Sec. III A, we focus on the case in which there is a large hierarchy between the momenta running in the loop and the external ones while in Sec. III B we consider the case in which the external momenta are generic. In Sec. IV, we discuss the implications of the perturbative bound in Eq. (1). In particular, in Sec. IV A, we consider the case in which

the external momenta are long CMB modes. In this section, we critically compare our result with those of Ref. [35], and discuss a number of crucial generalization. In Sec. IV B, we extend the computation to the case in which the external momenta are short modes. Finally, we conclude in Sec. V.

II. SETUP OF THE COMPUTATION USING THE “IN-IN” FORMALISM

A. Conventions

First, we set our conventions. We set the reduced Planck mass to one; t is the cosmic time (with $' \equiv d/dt$) and τ the conformal time (with $' \equiv d/d\tau$) with $dt/d\tau = a$ being a the scale factor of the flat Friedmann-Lemaître-Robertson-Walker (FLRW) metric $ds^2 = dt^2 - a^2(t)d\vec{x}^2$, with \vec{x} comoving coordinates. The Hubble rate is $H \equiv \dot{a}/a$. The e -fold time N is defined by $dN = Hdt$ from which we also have $dN/d\tau = aH$. The Hubble-flow parameters ϵ_i (for $i \geq 1$) are defined by the recursive relation

$$\epsilon_i \equiv \frac{\dot{\epsilon}_{i-1}}{H\epsilon_{i-1}}, \quad \text{with: } \epsilon_0 \equiv \frac{1}{H}. \quad (2)$$

As customary, we simply indicate as ϵ the first Hubble parameter, $\epsilon \equiv \epsilon_1 = -\dot{H}/H^2$. Instead of the second Hubble parameter ϵ_2 , sometimes it is useful to introduce the Hubble parameter η defined by¹

$$\eta \equiv -\frac{\ddot{H}}{2H\dot{H}} = \epsilon - \frac{1}{2} \frac{d \log \epsilon}{dN}, \quad \text{with: } \epsilon_2 = 2\epsilon - 2\eta. \quad (3)$$

We consider the theory described by the action

$$\mathcal{S} = \int d^4x \sqrt{-g} \left[\frac{1}{2} R(g) + \frac{1}{2} g^{\mu\nu} (\partial_\mu \phi)(\partial_\nu \phi) - V(\phi) \right]. \quad (4)$$

$R(g)$ is the scalar curvature associated with the space-time whose geometry is described by the metric g with line element $ds^2 = g_{\mu\nu} dx^\mu dx^\nu$. The classical background evolves in the flat FLRW universe and the background value of the scalar field is a function of time, $\phi(t)$. We tacitly assume that the scalar potential features an approximate stationary inflection point so as to trigger the transition SR/USR/SR.

We focus on scalar perturbations. We consider the perturbed metric in the following generic form

$$ds^2 = N^2 dt^2 - h_{ij}(N^i dt + dx^i)(N^j dt + dx^j), \quad (5)$$

and choose the gauge in which

¹We remark that in Ref. [35] the symbol η refers to the second Hubble parameter ϵ_2 .

$$\begin{aligned} N &= 1 + \delta N(\vec{x}, t), & N^i &= \delta^{ij} \partial_j B(\vec{x}, t), \\ h_{ij} &= a^2(t) e^{2\zeta(\vec{x}, t)} \delta_{ij}, & \delta\phi(\vec{x}, t) &= 0. \end{aligned} \quad (6)$$

The field $\zeta(\vec{x}, t)$ is the only independent scalar degree of freedom since N and N^i are Lagrange multipliers subject to the momentum and Hamiltonian constraints. It is important to stress that the variable ζ as defined in Eq. (6) is constant outside the horizon (more in general, outside the horizon and after the end of possible nonadiabatic phases) and represents the correct nonlinear generalization of the Bardeen variable [45].

At the quadratic order in the fluctuations, the action is

$$S_2 = \int d^4x e a^3 \left[\dot{\zeta}^2 - \frac{(\partial_k \zeta)(\partial^k \zeta)}{a^2} \right]. \quad (7)$$

Comoving curvature perturbations are quantized by introducing the free operator

$$\begin{aligned} \hat{\zeta}(\vec{x}, \tau) &= \int \frac{d^3\vec{k}}{(2\pi)^3} \hat{\zeta}(\vec{k}, \tau) e^{i\vec{x}\cdot\vec{k}}, \quad \text{with} \\ \hat{\zeta}(\vec{k}, \tau) &= \zeta_k(\tau) a_{\vec{k}} + \zeta_k^*(\tau) a_{-\vec{k}}^\dagger, \end{aligned} \quad (8)$$

and

$$\begin{aligned} [a_{\vec{k}}, a_{\vec{k}'}] &= [a_{\vec{k}}^\dagger, a_{\vec{k}'}^\dagger] = 0, & [a_{\vec{k}}, a_{\vec{k}'}^\dagger] &= (2\pi)^3 \delta^{(3)}(\vec{k} - \vec{k}'), \\ a_{\vec{k}}|0\rangle &= 0, \end{aligned} \quad (9)$$

where the last condition defines the vacuum of the free theory $|0\rangle$. We define the comoving wave number $k \equiv |\vec{k}|$. The scale factor in the FLRW universe corresponds to a rescaling of the spatial coordinate; consequently, physically sensible results should be invariant under the rescaling [46]

$$a \rightarrow \lambda a, \quad \vec{x} \rightarrow \vec{x}/\lambda, \quad \vec{k} \rightarrow \lambda \vec{k}, \quad k \rightarrow |\lambda| k, \quad \text{with } \lambda \in \mathbb{R}. \quad (10)$$

Furthermore, if we consider the conformal time τ instead of the cosmic time t , we also have

$$\tau \rightarrow \tau/\lambda. \quad (11)$$

Notice that, under the above rescaling, we have $a_{\vec{k}} \rightarrow a_{\vec{k}}/|\lambda|^{3/2}$ (from the scaling property of the three-dimensional δ function) and, consequently, $\zeta_k \rightarrow \zeta_k/|\lambda|^{3/2}$ so that $\hat{\zeta}(\vec{k}, \tau) \rightarrow \hat{\zeta}(\vec{k}, \tau)/|\lambda|^3$ and $\hat{\zeta}(\vec{x}, \tau)$ invariant. In the case of free fields, we have

$$\begin{aligned} \langle 0 | \hat{\zeta}(\vec{k}_1, \tau_1) \hat{\zeta}(\vec{k}_2, \tau_2) | 0 \rangle \\ = (2\pi)^3 \delta(\vec{k}_1 + \vec{k}_2) \zeta_{k_1}(\tau_1) \zeta_{k_2}^*(\tau_2). \end{aligned} \quad (12)$$

In the presence of a time derivative, we simply have

$$\begin{aligned} \langle 0 | \hat{\zeta}'(\vec{k}_1, \tau_1) \hat{\zeta}(\vec{k}_2, \tau_2) | 0 \rangle \\ = (2\pi)^3 \delta(\vec{k}_1 + \vec{k}_2) \zeta'_{k_1}(\tau_1) \zeta_{k_2}^*(\tau_2). \end{aligned} \quad (13)$$

Note that the time dependence occurs in the mode function, not in the raising/lowering operator. The mode function $\zeta_k(\tau)$ is related to the linear-order Mukhanov-Sasaki (M-S) equation. More in detail, if we define $\zeta_k(\tau) = u_k(\tau)/z(\tau)$ with $z(\tau) \equiv a(\tau)\sqrt{2\epsilon(\tau)}$, the mode $u_k(\tau)$ verifies the equation

$$\frac{d^2 u_k}{d\tau^2} + \left(k^2 - \frac{1}{z} \frac{d^2 z}{d\tau^2} \right) u_k = 0. \quad (14)$$

We are interested in the computation of the quantity

$$\lim_{\tau \rightarrow 0^-} \langle \hat{\zeta}(\vec{x}_1, \tau) \hat{\zeta}(\vec{x}_2, \tau) \rangle = \int \frac{d^3\vec{k}}{(2\pi)^3} P(k) e^{i\vec{k}\cdot(\vec{x}_1 - \vec{x}_2)}, \quad (15)$$

at some late time $\tau \rightarrow 0^-$ at which curvature perturbations become constant at superhorizon scales. Equivalently, we write

$$\begin{aligned} \lim_{\tau \rightarrow 0^-} \langle \hat{\zeta}(\vec{x}, \tau) \hat{\zeta}(\vec{x}, \tau) \rangle &= \int \frac{dk}{k} \underbrace{\left[\frac{k^3}{2\pi^2} P(k) \right]}_{\equiv \mathcal{P}(k)} \\ &= \int \frac{dk}{k} \mathcal{P}(k), \end{aligned} \quad (16)$$

where $\mathcal{P}(k)$ is the a -dimensional power spectrum. At the level of the quadratic action, we find

$$\begin{aligned} \langle 0 | \hat{\zeta}(\vec{x}_1, \tau) \hat{\zeta}(\vec{x}_2, \tau) | 0 \rangle \\ = \int \frac{d^3\vec{k}_1}{(2\pi)^3} d^3\vec{k}_2 \delta(\vec{k}_1 + \vec{k}_2) \zeta_{k_1}(\tau) \zeta_{k_2}^*(\tau) e^{i(\vec{x}_1 \cdot \vec{k}_1 + \vec{x}_2 \cdot \vec{k}_2)} \\ = \int \frac{d^3\vec{k}}{(2\pi)^3} |\zeta_k(\tau)|^2 e^{i\vec{k}\cdot(\vec{x}_1 - \vec{x}_2)}, \end{aligned} \quad (17)$$

which of course gives the familiar result

$$\mathcal{P}(k) = \lim_{\tau \rightarrow 0^-} \frac{k^3}{2\pi^2} |\zeta_k(\tau)|^2. \quad (18)$$

The goal is to compute corrections that arise from the presence of interactions. This means that, in Eq. (15), the vacuum expectation value should refer to the vacuum $|\Omega\rangle$ of the interacting theory and the dynamics of the operator $\hat{\zeta}(\vec{x}, \tau)$ is described by the full action that also includes interactions.

We compute the left-hand side of Eq. (15) by means of the “*in-in*” formalism (see, e.g., [47–49]). Correlators are given by

$$\begin{aligned} \langle \Omega | \hat{\mathcal{O}}(\tau) | \Omega \rangle &\equiv \langle \hat{\mathcal{O}}(\tau) \rangle \\ &= \langle 0 | \left\{ \bar{T} \exp \left[i \int_{-\infty(1+i\epsilon)}^{\tau} d\tau' \hat{H}_{\text{int}}(\tau') \right] \right\} \\ &\quad \times \hat{\mathcal{O}}_I(\tau) \left\{ T \exp \left[-i \int_{-\infty(1-i\epsilon)}^{\tau} d\tau' \hat{H}_{\text{int}}(\tau') \right] \right\} | 0 \rangle, \end{aligned} \quad (19)$$

where on the right-hand side all fields appearing in $\hat{\mathcal{O}}_I(\tau)$ and $\hat{H}_{\text{int}}(\tau')$ are free fields in the interaction picture. We shall indicate free fields in the interaction picture with the additional subscript $_I$. It should be noted that the latter are nothing but the operators of the free theory that we quantized in Eq. (8).

T and \bar{T} are the time and antitime ordering operator, respectively. As customary, the small imaginary deformation in the integration contour guarantees that $|\Omega\rangle \rightarrow |0\rangle$ as $\tau \rightarrow -\infty$ where $|\Omega\rangle$ is the vacuum of the interacting theory. On the left-hand side, the operator $\hat{\mathcal{O}}(\tau)$ is the equal-time product of operators at different space points, precisely like in Eq. (15). We expand in the interaction Hamiltonian, so we use the Dyson series

$$\begin{aligned} T \exp \left[-i \int_{-\infty_-}^{\tau} d\tau' \hat{H}_{\text{int}}(\tau') \right] \\ = 1 - i \int_{-\infty_-}^{\tau} d\tau' \hat{H}_{\text{int}}(\tau') \\ + i^2 \int_{-\infty_-}^{\tau} d\tau' \int_{-\infty_-}^{\tau'} d\tau'' \hat{H}_{\text{int}}(\tau') \hat{H}_{\text{int}}(\tau'') + \dots, \end{aligned} \quad (20)$$

where, for simplicity, we introduce the short-hand notation $\infty_{\pm} \equiv \infty(1 \pm i\epsilon)$. Each order in \hat{H}_{int} is an interaction vertex, and carries both a time integral and the space integral (enclosed in the definition of \hat{H}_{int}) which in Fourier space enforces momentum conservation.

It is crucial to correctly identify the interaction Hamiltonian. Before proceeding in this direction, let us clarify our notation. We expand the action in the form

$$\begin{aligned} \mathcal{S} &= \int d^3\vec{x} dt \underbrace{\mathcal{L}[\zeta(\vec{x}, t), \dot{\zeta}(\vec{x}, t), \partial_k \zeta(\vec{x}, t)]}_{\equiv \mathcal{L}[\zeta(\vec{x}, t)]} \\ &= \underbrace{\int d^3\vec{x} dt \mathcal{L}_2(\vec{x}, t)}_{\equiv S_2} + \underbrace{\int d^3\vec{x} dt \mathcal{L}_3[\zeta(\vec{x}, t)]}_{\equiv S_3} \\ &\quad + \underbrace{\int d^3\vec{x} dt \mathcal{L}_4[\zeta(\vec{x}, t)]}_{\equiv S_4} + \dots, \end{aligned} \quad (21)$$

with S_2 defined in Eq. (7). We also define (as a function of conformal time)

$$\begin{aligned} H_{\text{int}}^{(k)}(\tau) &\equiv \int d^3\vec{x} \mathcal{H}_k[\zeta(\vec{x}, \tau)] \\ \Rightarrow \hat{H}_{\text{int}}^{(k)}(\tau) &\equiv \int d^3\vec{x} \mathcal{H}_k[\hat{\zeta}_I(\vec{x}, \tau)]. \end{aligned} \quad (22)$$

At the cubic order, we simply have

$$\mathcal{H}_3[\zeta(\vec{x}, \tau)] = -\mathcal{L}_3[\zeta(\vec{x}, \tau)]. \quad (23)$$

We shall construct the relevant cubic interaction Hamiltonian in Sec. II C. At the quartic order, simply writing $\mathcal{H}_4 = -\mathcal{L}_4$ does not capture the correct result if the cubic Lagrangian features interactions that depend on the time derivative of ζ since the latter modify the definition of the conjugate momentum.

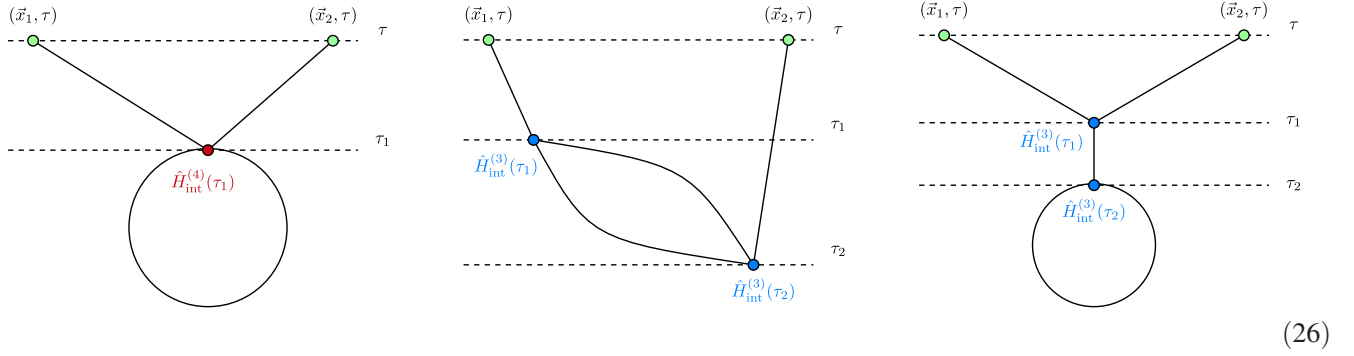
Using, at the operator level, the notation introduced in Eq. (22), we schematically write at the first order in the Dyson series expansion

$$\begin{aligned} \langle \hat{\zeta}(\vec{x}_1, \tau) \hat{\zeta}(\vec{x}_2, \tau) \rangle_{1^{\text{st}}} \\ = \langle 0 | \hat{\zeta}_I(\vec{x}_1, \tau) \hat{\zeta}_I(\vec{x}_2, \tau) \left[-i \int_{-\infty_-}^{\tau} d\tau' \hat{H}_{\text{int}}^{(4)}(\tau') \right] | 0 \rangle \\ + \langle 0 | \left[i \int_{-\infty_+}^{\tau} d\tau' \hat{H}_{\text{int}}^{(4)}(\tau') \right] \hat{\zeta}_I(\vec{x}_1, \tau) \hat{\zeta}_I(\vec{x}_2, \tau) | 0 \rangle. \end{aligned} \quad (24)$$

At the first order, therefore, the first nonzero quantum correction involves the quartic Hamiltonian. At the second order in the Dyson series expansion and considering again terms with up to eight fields in the vacuum expectation values, we write schematically

$$\begin{aligned} \langle \hat{\zeta}(\vec{x}_1, \tau) \hat{\zeta}(\vec{x}_2, \tau) \rangle_{2^{\text{nd}}} &= \langle 0 | \hat{\zeta}_I(\vec{x}_1, \tau) \hat{\zeta}_I(\vec{x}_2, \tau) \left[- \int_{-\infty_-}^{\tau} d\tau' \int_{-\infty_-}^{\tau'} d\tau'' \hat{H}_{\text{int}}^{(3)}(\tau') \hat{H}_{\text{int}}^{(3)}(\tau'') \right] | 0 \rangle \\ &\quad + \langle 0 | \left[- \int_{-\infty_+}^{\tau} d\tau' \int_{-\infty_+}^{\tau'} d\tau'' \hat{H}_{\text{int}}^{(3)}(\tau'') \hat{H}_{\text{int}}^{(3)}(\tau') \right] \hat{\zeta}_I(\vec{x}_1, \tau) \hat{\zeta}_I(\vec{x}_2, \tau) | 0 \rangle \\ &\quad + \langle 0 | \left[i \int_{-\infty_+}^{\tau} d\tau' \hat{H}_{\text{int}}^{(3)}(\tau') \right] \hat{\zeta}_I(\vec{x}_1, \tau) \hat{\zeta}_I(\vec{x}_2, \tau) \left[-i \int_{-\infty_-}^{\tau} d\tau'' \hat{H}_{\text{int}}^{(3)}(\tau'') \right] | 0 \rangle. \end{aligned} \quad (25)$$

The vacuum expectation values of interacting-picture fields can be computed using Wick's theorem. Schematically, Eqs. (24), (25) give rise to the following connected diagrams.



From the above classification, we see that, at the same loop order, we have three classes of connected diagrams that, in principle, should be discussed together. Notice that, contrary to the first two, the last diagram is not of 1-particle-irreducible (1PI) type since it consists of a tadpole attached to a two-point propagator.

To proceed further, we need to specify the background dynamics, that shape the time evolution of the Hubble parameters, and the interaction Hamiltonian, that specifies which terms in the Dyson expansion contribute at a given perturbative order.

B. The (minimal) dynamics of ultraslow-roll

We start with a discussion of the USR dynamics. In order to make our discussion more concrete, in the following we shall refer to Fig. 1, see the caption for details. In this figure, we plot both the classical (top panel) and quantum (bottom panel) dynamics that characterize a realistic model of single-field inflation that features a phase of USR because of the presence of an approximate stationary inflection point in the inflationary potential. We refer to Ref. [12] for more details about the model; we remark that this model, without including loop corrections to the computation of the curvature power spectrum, is compatible with CMB constraints and gives $\approx 100\%$ of dark matter in the form of asteroid-mass PBHs.² In Fig. 1, the relation between e -fold time N (bottom x axis) and conformal time τ (top x axis) is given by the integral

$$\tau = -\frac{1}{k_\star} \int_N^{N_0} \frac{H(N_\star)}{H(N')} e^{N_\star - N'} dN', \quad (27)$$

where N_0 indicates the end of inflation, with τ conventionally set to 0 at this time, and N_\star the instant of time at which the comoving scale $k_\star = 0.05 \text{ Mpc}^{-1}$ crosses the Hubble horizon. In Fig. 1, we set $N_\star = 0$, and the model

²The model predicts the tensor-to-scalar ratio $r \simeq 0.037$ which is still (barely) compatible, at 95% confidence level, with the latest results released by the BICEP and Keck collaboration [50].

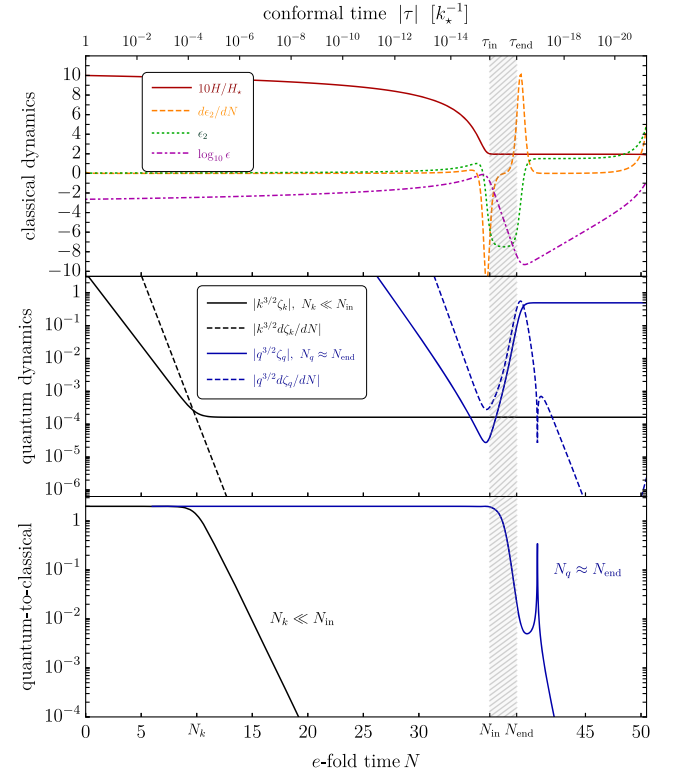


FIG. 1. Classical (top panel) and quantum (central panel) dynamics in the context of an explicit single-field model of inflation that exhibits the presence of a phase of USR in between the time interval $N_{\text{in}} < N < N_{\text{end}}$ (cf. Ref. [12]). In this specific realization, we have $N_{\text{in}} = 36.3$ and $N_{\text{end}} = 38.8$. Top panel: we plot the evolution of the background quantities ϵ , ϵ_2 and ϵ'_2 [cf. Eqs. (2), (3)] together with the evolution of the Hubble rate (normalized with respect to the value $H_\star \equiv H(N_\star)$ and scaled by a factor of 10 for ease of comparison). Central panel: we plot the solutions of the M-S equation in Eq. (33) for two different curvature modes. The mode in black (blue) exits the Hubble horizon well before (during) the USR phase. Bottom panel: we plot the classically parameter C_k for the same two modes (cf. the main text for details). In the case of the black mode ($N_k \ll N_{\text{in}}$) the classically parameter quickly vanishes after horizon crossing, and remains negligible also during the USR phase. In the case of the blue mode ($N_q \approx N_{\text{end}}$) the classically parameter remains sizable during the USR phase, signaling that this mode retains its quantum nature during USR.

gives $N_0 - N_\star \simeq 52$. We can highlight few crucial properties of the dynamics presented above:

- (1) We start from the classical analysis. During USR, $\epsilon_2(\tau)$ changes according to the schematic

$$\epsilon_2 \approx 0 \xRightarrow{\text{SR/USR at time } \tau_{\text{in}}} |\epsilon_2| > 3 \xRightarrow{\text{USR/SR at time } \tau_{\text{end}}} \epsilon_2 \approx O(1), \quad (28)$$

thus making $\epsilon'_2(\tau)$ nonzero at around the two transitions at conformal times τ_{in} and τ_{end} (equivalently, at e -fold times N_{in} and N_{end}). The evolution of ϵ_2 and ϵ'_2 are shown in the top panel of Fig. 1, with dotted green and dashed orange lines, respectively.

- (2) During USR, the Hubble parameter ϵ decreases exponentially fast (the inflaton almost stops its classical motion). The evolution of ϵ is shown in the top panel of Fig. 1 (dot-dashed magenta line); in addition, we also plot the time evolution of the Hubble rate H .
- (3) We now consider the USR dynamics at the quantum level. It is crucial to understand the typical behavior of curvature modes (solid lines in the central panel of Fig. 1) and their time derivatives (dashed lines). In the central panel of Fig. 1, we plot two representative cases: the black lines correspond to the case of a mode ζ_k that exits the Hubble horizon at some time N_k well before the USR phase (like a CMB mode) while the blue lines correspond to a curvature mode ζ_q that exits the Hubble horizon at some time N_q during the USR phase. We notice that the derivative

$|d\zeta_k/dN|$ decays exponentially fast, and, soon after horizon crossing, becomes negligible, while $|\zeta_k|$ settles to a constant value. Consequently, we expect that interaction terms that involve the time derivative of CMB modes will be strongly suppressed.

- (4) Finally, we consider the issue of the quantum-to-classical transition. We define the so-called classicality parameter [51] $C_k = |\zeta_k \dot{\zeta}_k^* - \zeta_k^* \dot{\zeta}_k| / |\zeta_k \dot{\zeta}_k|$, which goes to zero in the classical limit. In the case of conventional SR dynamics, the classicality parameter scales according to $C_k \sim 2k\tau$, and it vanishes exponentially fast right after the horizon crossing time. In the bottom panel of Fig. 1, we plot the classicality parameter for two representative modes of our dynamics. The black modes experiences its horizon crossing well before the USR phase ($N_k \ll N_{\text{in}}$). Its classicality parameter quickly vanishes and remains $\ll 1$ during the subsequent USR phase. The blue line, on the contrary, represents the classicality parameter for a mode that experiences its horizon crossing during the USR phase. Its classicality parameter remains sizable during the USR phase, signalling that this short mode can not be treated classically during USR.

With the aim of facilitating the numerical computations of the following sections, instead of working with a numerical description of USR, we now introduce a simple semianalytical model [52–54]. We define the hyperbolic tangent parametrization

$$\eta(N) = \frac{1}{2} \left[-\eta_{\text{II}} + \eta_{\text{II}} \tanh\left(\frac{N - N_{\text{in}}}{\delta N}\right) \right] + \frac{1}{2} \left[\eta_{\text{II}} + \eta_{\text{III}} + (\eta_{\text{III}} - \eta_{\text{II}}) \tanh\left(\frac{N - N_{\text{end}}}{\delta N}\right) \right], \quad (29)$$

where the parameter δN controls the width of the two transitions at N_{in} and N_{end} . The limit $\delta N \rightarrow 0$ reproduces the step-function approximation. Using the definition

$$\delta(x) = \lim_{\epsilon \rightarrow 0} \frac{1}{2\epsilon \cosh^2(x/\epsilon)}, \quad (30)$$

we find

$$\lim_{\delta N \rightarrow 0} \frac{d\eta}{dN} = (-\eta_{\text{II}} + \eta_{\text{III}}) \delta(N - N_{\text{end}}) + \eta_{\text{II}} \delta(N - N_{\text{in}}). \quad (31)$$

Using $\eta \simeq -(1/2)d \log \epsilon / dN$, we find the following expression

$$\begin{aligned} \frac{\epsilon(N)}{\epsilon_{\text{ref}}} &= e^{-\eta_{\text{III}}(N - N_{\text{ref}})} \left[\cosh\left(\frac{N - N_{\text{end}}}{\delta N}\right) \cosh\left(\frac{N - N_{\text{in}}}{\delta N}\right) \right]^{-\frac{\delta N \eta_{\text{III}}}{2}} \left[\cosh\left(\frac{N_{\text{ref}} - N_{\text{end}}}{\delta N}\right) \cosh\left(\frac{N_{\text{ref}} - N_{\text{in}}}{\delta N}\right) \right]^{\frac{\delta N \eta_{\text{III}}}{2}} \\ &\times \left[\cosh\left(\frac{N - N_{\text{end}}}{\delta N}\right) \text{sech}\left(\frac{N - N_{\text{in}}}{\delta N}\right) \right]^{\delta N (\eta_{\text{II}} - \frac{\eta_{\text{III}}}{2})} \left[\cosh\left(\frac{N_{\text{ref}} - N_{\text{end}}}{\delta N}\right) \text{sech}\left(\frac{N_{\text{ref}} - N_{\text{in}}}{\delta N}\right) \right]^{\frac{\delta N}{2} (-2\eta_{\text{II}} + \eta_{\text{III}})}, \end{aligned} \quad (32)$$

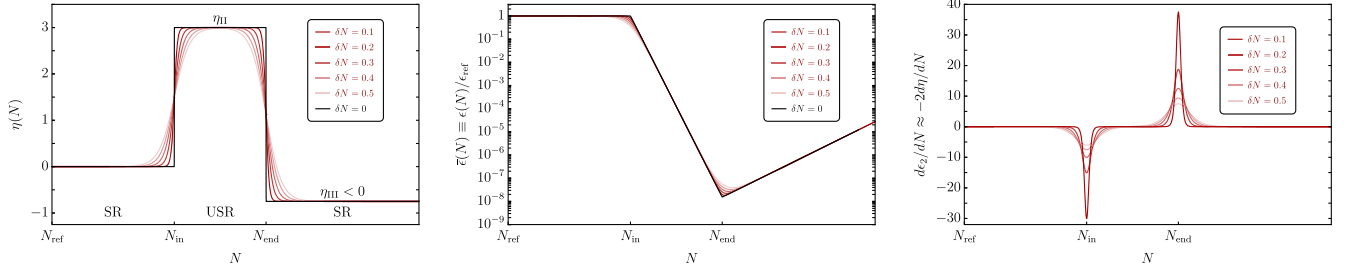


FIG. 2. Schematic evolution of $\eta(N)$ in Eq. (29) (left panel), $\epsilon(N)$ in Eq. (32) (central panel) and $d\epsilon_2/dN$ (right panel) as function of the number of e -folds N . We explore different values of δN with the limit $\delta N \rightarrow 0$ that corresponds to instantaneous transitions SR/USR at $N = N_{\text{in}}$ and USR/SR at $N = N_{\text{end}}$. In the right panel, the limit $\delta N \rightarrow 0$ corresponds to δ function transitions at N_{in} and N_{end} . Furthermore, notice that the lines corresponding to $d\epsilon_2/dN$ and $-2d\eta/dN$ superimpose, showing that $-2d\eta/dN$ is a perfect approximation of $d\epsilon_2/dN$.

where $\epsilon_{\text{ref}} \ll 1$ is the value of ϵ at some initial reference time N_{ref} . For future reference, we define $\bar{\epsilon}(N) \equiv \epsilon(N)/\epsilon_{\text{ref}}$. In this way we have an analytical description of the background dynamics; most importantly, Eqs. (29), (32) are almost all that we need to know to solve the M-S equation [55,56]

$$\frac{d^2 u_k}{dN^2} + (1 - \epsilon) \frac{du_k}{dN} + \left[\frac{k^2}{(aH)^2} + (1 + \epsilon - \eta)(\eta - 2) - \frac{d}{dN}(\epsilon - \eta) \right] u_k = 0. \quad (33)$$

For consistency with Eq. (32), we consider the Hubble rate as a function of time according to

$$H(N) = H(N_{\text{ref}}) \exp \left[- \int_{N_{\text{ref}}}^N \epsilon(N') dN' \right]. \quad (34)$$

We shall use the short-hand notation $a(N_i) \equiv a_i$ and $H(N_i) \equiv H_i$. Consequently, we rewrite Eq. (33) in the form

$$\frac{d^2 u_k}{dN^2} + (1 - \epsilon) \frac{du_k}{dN} + \left[\bar{k}^2 \left(\frac{H_{\text{in}}}{H} \right)^2 e^{2(N_{\text{in}} - N)} + (1 + \epsilon - \eta)(\eta - 2) - \frac{d}{dN}(\epsilon - \eta) \right] u_k = 0, \quad (35)$$

with $\bar{k} \equiv k/(a_{\text{in}} H_{\text{in}})$. We solve the above equation for different \bar{k} with Bunch-Davies initial conditions

$$\sqrt{k} u_k(N) = \frac{1}{\sqrt{2}}, \quad \sqrt{k} \frac{du_k}{dN}(N) = -\frac{i}{\sqrt{2}} \frac{k}{a(N)H(N)}, \quad (36)$$

at some arbitrary time $N \ll N_k$ with $k = a(N_k)H(N_k)$. Modes with $\bar{k} \approx O(1)$ are modes that exit the Hubble horizon at about the beginning of the USR phase, modes with $\bar{k} \ll 1$ are modes that exit the Hubble horizon well before the beginning of the USR phase, modes with $\bar{k} \gg 1$ are modes that exit the Hubble horizon well after the beginning of the USR phase. In the left panel of Fig. 3, we show the tree-level power spectrum that we obtain by numerically solving Eq. (35) and using Eq. (18). Thanks to our parametrization in Eq. (29) we control the sharpness of the transition varying δN .

In order to make contact with the analysis of Ref. [35], we set $\eta_{\text{III}} = 0$. However, it should be noted that in more realistic models we need $\eta_{\text{III}} \neq 0$ and negative so that the power spectrum decreases for modes with $\bar{k} \gg 1$. This

feature is necessary if we want to connect the USR phase to a subsequent SR phase that ends inflation. Since we are considering single-field models of inflation, in our analysis this is a necessary requirement. Consequently, the power spectrum at small scales—both before and after the peak—does not respect the property of scale invariance. Before the peak, the power spectrum of the short modes grows with a maximum slope given by $\mathcal{P}(\bar{k}) \sim \bar{k}^4$; after the peak, the power spectrum of the short modes decays approximately as $\mathcal{P}(\bar{k}) \sim \bar{k}^{2\eta_{\text{III}}}$. After the peak, therefore, the power spectrum becomes approximately scale invariant only if we take $\eta_{\text{III}} \approx 0$; however, in such case ϵ remains anchored to the tiny value reached during the USR phase and inflation never ends.

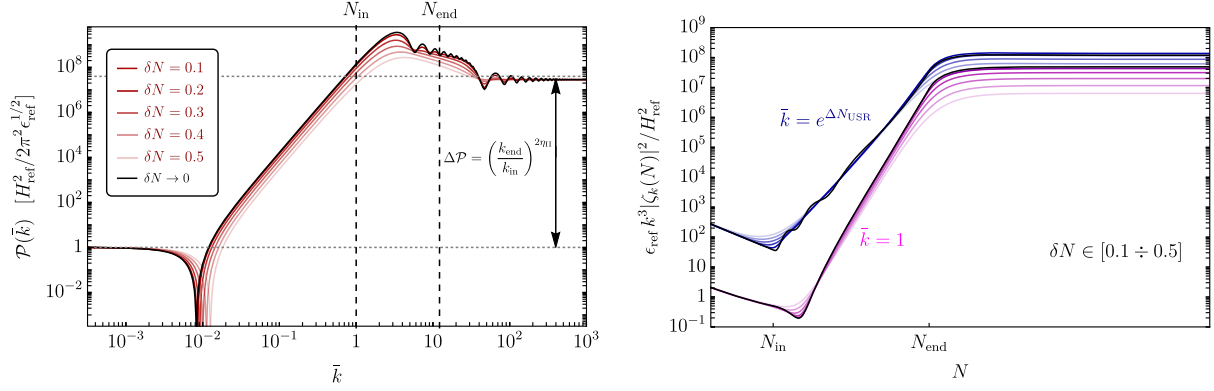


FIG. 3. Left panel: tree-level power spectrum in the minimal dynamics of Sec. II B. The numerical values of the other parameters are $\eta_{\text{II}} = 3.5$, $\eta_{\text{III}} = 0$ and $N_{\text{end}} - N_{\text{in}} = 2.5$. In our parametrization, we go beyond the instantaneous transition approximation and we explore different values of δN . The vertical double-arrow indicates the growth of the power spectrum given by the naïve scaling $\Delta \mathcal{P} = (k_{\text{end}}/k_{\text{in}})^{2\eta_{\text{III}}} = e^{2\eta_{\text{III}}\Delta N_{\text{USR}}}$. This scaling captures well the amplitude of the transition from the initial to the final SR phase but it does not give a reliable estimate of the peak amplitude of the power spectrum, which can easily be one order of magnitude larger. Right panel: time evolution of two representative modes with $\bar{k} = 1$ and $\bar{k} = e^{\Delta N_{\text{USR}}}$ for $\delta N \in [0.1 \div 0.5]$ (from darker to lighter colors, respectively). The black lines represent the limit $\delta N \rightarrow 0$.

In Ref. [35], the loop integration is restricted to the interval of modes $\bar{k} \in [\bar{k}_{\text{in}}, \bar{k}_{\text{end}}]$, where $\bar{k}_{\text{in}} = 1$ and $\bar{k}_{\text{end}} = e^{\Delta N_{\text{USR}}}(H_{\text{end}}/H_{\text{in}}) \simeq e^{\Delta N_{\text{USR}}}$ with $\Delta N_{\text{USR}} \equiv N_{\text{end}} - N_{\text{in}}$. This interval of modes is limited by the two vertical dashed lines in the left panel of Fig. 3. In Ref. [35], limiting the integration to the range $\bar{k} \in [\bar{k}_{\text{in}}, \bar{k}_{\text{end}}]$ is justified by the fact that the power spectrum of short modes peaks in this window of modes.

For future reference, let us stress one more important point. In the left panel of Fig. 3 we indicate the growth of the power spectrum given by the scaling $\Delta \mathcal{P} = (k_{\text{end}}/k_{\text{in}})^{2\eta_{\text{III}}}$. This result immediately follows from the application of the SR formula $\mathcal{P}(k) = H^2/8\pi^2\epsilon$ if one accounts for the exponential decay $\epsilon \sim e^{-2\eta_{\text{III}}N}$ during USR and converts N into k by means of the horizon-crossing condition $k = aH$. Therefore, not surprisingly, the scaling $\Delta \mathcal{P} = (k_{\text{end}}/k_{\text{in}})^{2\eta_{\text{III}}}$ captures well the growth of the power spectrum if one directly jumps from the initial to the final SR phase. However, as shown in the left panel of Fig. 3, the above estimate does not

accurately describe the amplitude of the power spectrum at the position of its peak; the latter can easily be one order of magnitude larger than what suggested by $\Delta \mathcal{P} = (k_{\text{end}}/k_{\text{in}})^{2\eta_{\text{III}}}$. This feature has important consequences when estimating the PBH abundance, which is rather sensitive to the spectral amplitude. We will come back to this point in the next section.

Finally, it is possible to check numerically that neglecting the time dependence of the Hubble rate as in Eq. (34) has a negligible impact. In the following, therefore, we shall keep H constant (that is, $H = H_{\text{ref}}$ does not evolve in time). Furthermore, if we take H constant and in the limit $\delta N = 0$, it is possible to get, for some special values of η_{II} and η_{III} , a complete analytical description of the SR/USR/SR dynamics [12,52].

C. The cubic action

At the cubic order in the fluctuations, the action is

$$\begin{aligned} \mathcal{S}_3 = \int d^4x \Big\{ & \epsilon^2 a^3 \dot{\zeta}^2 \zeta + \epsilon^2 a \zeta (\partial_k \zeta) (\partial^k \zeta) - 2\epsilon^2 a^3 \dot{\zeta} (\partial_k \zeta) \partial^k (\partial^{-2} \dot{\zeta}) + \frac{\epsilon \dot{\epsilon}_2}{2} a^3 \dot{\zeta} \zeta^2 - \frac{a^3 \epsilon^3}{2} [\dot{\zeta}^2 \zeta - \zeta \partial_k \partial_l (\partial^{-2} \dot{\zeta}) \partial^k \partial^l (\partial^{-2} \dot{\zeta})] \\ & + \left[\frac{d}{dt} (\epsilon a^3 \dot{\zeta}) - \epsilon a \partial_k \partial^k \zeta \right] \left[\frac{\epsilon_2}{2} \zeta^2 + \frac{2}{H} \dot{\zeta} \zeta - \frac{1}{2a^2 H^2} (\partial_k \zeta) (\partial^k \zeta) + \frac{1}{2a^2 H^2} \partial^{-2} \partial_k \partial_l (\partial^k \zeta \partial^l \zeta) \right. \\ & \left. + \frac{\epsilon}{H} (\partial_k \zeta) \partial^k (\partial^{-2} \dot{\zeta}) - \frac{\epsilon}{H} \partial^{-2} \partial_k \partial_l \partial^k \zeta \partial^l (\partial^{-2} \dot{\zeta}) \right] \Big\}. \end{aligned} \quad (37)$$

As shown in Ref. [45], it is possible to simplify the cubic action by means of a field redefinition that introduces a non-linear shift in the original field. Concretely, if we define

$$\zeta \equiv \zeta_n + f(\zeta_n), \quad (38)$$

with

$$f(\zeta) \equiv \frac{1}{2} \left[\frac{\epsilon_2}{2} \zeta^2 + \frac{2}{H} \dot{\zeta} \zeta - \frac{(\partial_k \zeta)(\partial^k \zeta)}{2a^2 H^2} + \frac{1}{2a^2 H^2} \partial^{-2} \partial_k \partial_l (\partial^k \zeta \partial^l \zeta) + \frac{\epsilon}{H} (\partial_k \zeta) \partial^k (\partial^{-2} \dot{\zeta}) - \frac{\epsilon}{H} \partial^{-2} \partial_k \partial_l \partial^k \zeta \partial^l (\partial^{-2} \dot{\zeta}) \right], \quad (39)$$

we find, by direct computation, that at the quadratic order the field ζ_n is described by the action

$$\mathcal{S}_2(\zeta_n) = \int d^4x \epsilon a^3 \left[\dot{\zeta}_n^2 - \frac{(\partial_k \zeta_n)(\partial^k \zeta_n)}{a^2} \right], \quad (40)$$

which has the same structure as the quadratic action for the original variable ζ . However, at the cubic order, we find

$$\begin{aligned} \mathcal{S}_3(\zeta_n) = \int d^4x \left\{ \epsilon^2 a^3 \dot{\zeta}_n^2 \zeta_n + \epsilon^2 a \zeta_n (\partial_k \zeta_n) (\partial^k \zeta_n) - 2\epsilon^2 a^3 \dot{\zeta}_n (\partial_k \zeta_n) \partial^k (\partial^{-2} \dot{\zeta}_n) + \frac{\epsilon \dot{\epsilon}_2}{2} a^3 \dot{\zeta}_n \zeta_n^2 \right. \\ \left. - \frac{a^3 \epsilon^3}{2} [\dot{\zeta}_n^2 \zeta_n - \zeta_n \partial_k \partial_l (\partial^{-2} \dot{\zeta}_n) \partial^k \partial^l (\partial^{-2} \dot{\zeta}_n)] \right\}, \end{aligned} \quad (41)$$

in which, thanks to the above field redefinition, the second and third lines in Eq. (37) cancel out.

If we neglect terms with spatial derivatives and interactions suppressed by two or more powers of the Hubble parameter ϵ , then we find

$$\mathcal{S}_3(\zeta_n) \ni \int d^4x \frac{\epsilon \dot{\epsilon}_2}{2} a^3 \dot{\zeta}_n \zeta_n^2. \quad (42)$$

Notice that we do not count the coupling ϵ_2 as a slow-roll suppression since we are interested in the USR phase during which $|e_2| > 3$ and $\dot{\epsilon}_2 \neq 0$. Equation (42) is the only interaction included in Ref. [35]. This means that, implicitly, Ref. [35] computes the two-point function for the field ζ_n . This is because, in terms of the dynamical variable ζ , there is another interaction of order $\epsilon \epsilon_2$ that should be included, which is the one in the second line of Eq. (37).

However, as stressed in Ref. [45], ζ_n is not the right dynamical variable to consider since it is not conserved

outside the horizon. This is a trivial consequence of Eq. (38). Since ζ is conserved outside the horizon, ζ_n can not be conserved simply because various coefficients in the nonlinear relation in Eq. (38) are time dependent. Alternatively, as discussed in Ref. [45], the above fact is also evident from the very same structure of the interactions that appear in Eq. (41). The interaction $\epsilon \dot{\epsilon}_2 \dot{\zeta}_n \zeta_n^2$ only has one time derivative acting on the field ζ_n ; consequently, it alters the value of ζ_n on superhorizon scales (if one computes the equation of motion for ζ_n , it is easy to see that the constant solution is not stable). Let us make the above considerations more concrete. Eventually, we are interested in the computation of the two-point function for the original curvature field. Given the field redefinition in Eq. (38), we write

$$\begin{aligned} \langle \hat{\zeta}(\vec{x}_1, \tau) \hat{\zeta}(\vec{x}_2, \tau) \rangle &= \langle \{ \hat{\zeta}_n(\vec{x}_1, \tau) + f[\hat{\zeta}_n(\vec{x}_1, \tau)] \} \{ \hat{\zeta}_n(\vec{x}_2, \tau) + f[\hat{\zeta}_n(\vec{x}_2, \tau)] \} \rangle, \\ &= \langle \hat{\zeta}_n(\vec{x}_1, \tau) \hat{\zeta}_n(\vec{x}_2, \tau) \rangle + \end{aligned} \quad (43)$$

$$\langle \hat{\zeta}_n(\vec{x}_1, \tau) f[\hat{\zeta}_n(\vec{x}_2, \tau)] \rangle + \langle f[\hat{\zeta}_n(\vec{x}_1, \tau)] \hat{\zeta}_n(\vec{x}_2, \tau) \rangle + \quad (44)$$

$$\langle f[\hat{\zeta}_n(\vec{x}_1, \tau)] f[\hat{\zeta}_n(\vec{x}_2, \tau)] \rangle, \quad (45)$$

The first term, Eq. (43), corresponds to the two-point function for the shifted curvature field whose cubic action is given by Eq. (41); $\langle \hat{\zeta}_n(\vec{x}_1, \tau) \hat{\zeta}_n(\vec{x}_2, \tau) \rangle$ can be computed perturbatively by means of the “*in-in*” formalism sketched at the end of Sec. II A. Eqs. (44), (45) account for the difference between ζ and ζ_n at the nonlinear level. Notice that the first term in the functional form in Eq. (39) does not die off in the late-time limit $\tau \rightarrow 0^-$ (in which the power

spectrum must be eventually evaluated) if we consider the case in which $\epsilon_2 \neq 0$ after the USR phase (as expected in realistic single-field models, cf. Sec. II B). However, if we limit to the case in which $\eta_{\text{III}} = 0$ the contribution from the field redefinition vanishes. This limit was considered in Ref. [35]. In order to make contact with the analysis presented in Ref. [35], we shall also adopt in the bulk of this work the assumption $\eta_{\text{III}} = 0$.

Let us now come back to the schematic in Eq. (26). The cubic Hamiltonian interaction that follows from Eq. (42) gives rise to the last two topologies of connected diagrams illustrated in Eq. (26). As in Ref. [35], we will only focus on the 1PI diagram, that is, the central diagram in Eq. (26). The last diagram in Eq. (26) consists of a tadpole that is attached to a ζ propagator and affects at one-loop its two-point correlation function. The correct way to deal with tadpoles is by changing the background solution, cf. Ref. [57] for a discussion in the case of ordinary SR inflation and Ref. [46] for the case in which there are additional spectator fields. Recently, Ref. [58] estimated the tadpole correction to the background evolution in the context of a model in which there is a resonant amplification of field fluctuations. Imposing the condition that such modification is negligible could give rise to an additional perturbativity bound. We postpone a comprehensive exploration of this issue in the context of realistic USR dynamics to future work, cf. Sec. V.

D. Beyond the cubic action

Before proceeding, we comment about quartic interactions since, as qualitatively discussed in Eq. (26), they give rise to one-loop corrections which are of the same order if compared to those generated by cubic interaction terms. The derivation of the fourth-order action has been discussed in Ref. [59]. Based on this result, Refs. [35,37] claims that the relevant quartic interaction in the case of USR dynamics (that is, the quartic interaction proportional to ϵ_2) gives a vanishing contribution when inserted in Eq. (24). Reference [39] adopts an approach based on the effective field theory of inflation and includes cubic and quartic interactions. It finds that the latter gives a nontrivial contribution, and finds a loop-corrected power spectrum different from the one in Refs. [35,37]. It would be

important to perform a consistent comparison between these two approaches, including the full cubic and quartic interactions in both cases. Generally speaking, we expect cubic and quartic interactions to be inextricably linked. For instance, the quartic Hamiltonian receives a contribution that arises from the modification of the conjugate momentum if there are cubic interactions which depend on $\dot{\zeta}$. Similarly, cubic interactions with spatial derivatives are paired with quartic interactions induced by a residual spatial conformal symmetry of the perturbed metric [46]. En route, we notice that interactions with spatial derivatives are usually neglected for modes that are superhorizon. However, in the spirit of the loop computation in Ref. [35], the momenta over which the loop is integrated cross the horizon during the USR phase, and, naively, their spatial derivatives do not pay any superhorizon suppression.

In this work, as a preliminary step towards a more complete analysis and in order to compare our results with the claim made in Refs. [36–44], we only focus on the cubic interaction in Eq. (42). However, we stress that all the arguments listed above motivate the need for a more comprehensive analysis. We postpone this task to future work, cf. Sec. V.

III. ONE-LOOP COMPUTATION

We consider in this section the cubic interaction Hamiltonian given by (we omit the subscript I in the interaction-picture fields)

$$\hat{H}_{\text{int}}^{(3)}(\tau) = \frac{1}{2} \int d^3\vec{x} \epsilon(\tau) \epsilon'_2(\tau) a^2(\tau) \zeta'(\vec{x}, \tau) \zeta(\vec{x}, \tau)^2. \quad (46)$$

We consider Eq. (25); this can be written in the compact form

$$\langle \hat{\zeta}(\vec{x}_1, \tau) \hat{\zeta}(\vec{x}_2, \tau) \rangle_{2\text{nd}} = \langle \hat{\zeta}(\vec{x}_1, \tau) \hat{\zeta}(\vec{x}_2, \tau) \rangle_{2\text{nd}}^{(1,1)} - 2\text{Re}[\langle \hat{\zeta}(\vec{x}_1, \tau) \hat{\zeta}(\vec{x}_2, \tau) \rangle_{2\text{nd}}^{(0,2)}], \quad (47)$$

where

$$\langle \hat{\zeta}(\vec{x}_1, \tau) \hat{\zeta}(\vec{x}_2, \tau) \rangle_{2\text{nd}}^{(1,1)} \equiv \int_{-\infty(1+i\epsilon)}^{\tau} d\tau_1 \int_{-\infty(1-i\epsilon)}^{\tau} d\tau_2 \langle 0 | \hat{H}_{\text{int}}(\tau_1) \hat{\zeta}_I(\vec{x}_1, \tau) \hat{\zeta}_I(\vec{x}_2, \tau) \hat{H}_{\text{int}}(\tau_2) | 0 \rangle, \quad (48)$$

$$\langle \hat{\zeta}(\vec{x}_1, \tau) \hat{\zeta}(\vec{x}_2, \tau) \rangle_{2\text{nd}}^{(0,2)} \equiv \int_{-\infty(1-i\epsilon)}^{\tau} d\tau_1 \int_{-\infty(1-i\epsilon)}^{\tau_1} d\tau_2 \langle 0 | \hat{\zeta}_I(\vec{x}_1, \tau) \hat{\zeta}_I(\vec{x}_2, \tau) \hat{H}_{\text{int}}(\tau_1) \hat{H}_{\text{int}}(\tau_2) | 0 \rangle. \quad (49)$$

This expansion is consistent with Eq. (16) of Ref. [46]. Consider the first contribution in Eq. (48), one finds

$$\begin{aligned} \langle \hat{\zeta}(\vec{x}_1, \tau) \hat{\zeta}(\vec{x}_2, \tau) \rangle_{2\text{nd}}^{(1,1)} &= \frac{1}{4} \int_{-\infty_+}^{\tau} d\tau_1 \epsilon(\tau_1) \epsilon'_2(\tau_1) a^2(\tau_1) \int_{-\infty_-}^{\tau} d\tau_2 \epsilon(\tau_2) \epsilon'_2(\tau_2) a^2(\tau_2) \int d^3\vec{y} d^3\vec{z} \\ &\times \int \left[\prod_{i=1}^8 \frac{d^3\vec{k}_i}{(2\pi)^3} \right] e^{i\vec{y} \cdot (\vec{k}_1 + \vec{k}_2 + \vec{k}_3)} e^{i(\vec{x}_1 \cdot \vec{k}_4 + \vec{x}_2 \cdot \vec{k}_5)} e^{i\vec{z} \cdot (\vec{k}_6 + \vec{k}_7 + \vec{k}_8)} \\ &\times \langle 0 | \hat{\zeta}'_I(\vec{k}_1, \tau_1) \hat{\zeta}_I(\vec{k}_2, \tau_1) \hat{\zeta}_I(\vec{k}_3, \tau_1) \hat{\zeta}_I(\vec{k}_4, \tau) \hat{\zeta}_I(\vec{k}_5, \tau) \hat{\zeta}'_I(\vec{k}_6, \tau_2) \hat{\zeta}_I(\vec{k}_7, \tau_2) \hat{\zeta}_I(\vec{k}_8, \tau_2) | 0 \rangle. \end{aligned} \quad (50)$$

The 36 connected Wick contractions can be expressed as

$$\begin{aligned}
 \langle \hat{\zeta}(\vec{x}_1, \tau) \hat{\zeta}(\vec{x}_2, \tau) \rangle_{2\text{nd}}^{(1,1)} &= \int_{-\infty_+}^{\tau} d\tau_1 \epsilon(\tau_1) \epsilon'_2(\tau_1) a^2(\tau_1) \int_{-\infty_-}^{\tau} d\tau_2 \epsilon(\tau_2) \epsilon'_2(\tau_2) a^2(\tau_2) \int \frac{d^3 \vec{k}}{(2\pi)^3} \frac{d^3 \vec{q}}{(2\pi)^3} e^{i(\vec{x}_1 - \vec{x}_2) \cdot (\vec{k} + \vec{q})} \\
 &\times [|\zeta_{k+q}(\tau)|^2 \{ \zeta_k(\tau_1) \zeta'_{k+q}(\tau_1) \zeta_q(\tau_1) \zeta_k^*(\tau_2) \zeta'_{k+q}(\tau_2) \zeta_q^*(\tau_2) \\
 &+ \zeta_k(\tau_1) \zeta'_{k+q}(\tau_1) \zeta_q(\tau_1) \zeta_{k+q}^*(\tau_2) [\zeta_k^*(\tau_2) \zeta_q^*(\tau_2) + \zeta_k^*(\tau_2) \zeta_q^*(\tau_2)] \\
 &+ \zeta_k^*(\tau_2) \zeta'_{k+q}(\tau_2) \zeta_q^*(\tau_2) \zeta_{k+q}(\tau_1) [\zeta_k'(\tau_1) \zeta_q(\tau_1) + \zeta_k(\tau_1) \zeta_q'(\tau_1)] \\
 &+ \zeta_k'(\tau_1) \zeta_{k+q}(\tau_1) \zeta_q(\tau_1) \zeta_{k+q}^*(\tau_2) [\zeta_k^*(\tau_2) \zeta_q^*(\tau_2) + \zeta_k^*(\tau_2) \zeta_q^*(\tau_2)] \\
 &+ \zeta_k^*(\tau_2) \zeta_{k+q}^*(\tau_2) \zeta_q^*(\tau_2) \zeta_{k+q}(\tau_1) [\zeta_q(\tau_1) \zeta_k'(\tau_1) + \zeta_k(\tau_1) \zeta_q'(\tau_1)] \}.
 \end{aligned} \quad (51)$$

Consider now Eq. (49). One can write it in the form

$$\begin{aligned}
 \langle \hat{\zeta}(\vec{x}_1, \tau) \hat{\zeta}(\vec{x}_2, \tau) \rangle_{2\text{nd}}^{(0,2)} &= \frac{1}{4} \int_{-\infty_-}^{\tau} d\tau_1 \epsilon(\tau_1) \epsilon'_2(\tau_1) a^2(\tau_1) \int_{-\infty_-}^{\tau_1} d\tau_2 \epsilon(\tau_2) \epsilon'_2(\tau_2) a^2(\tau_2) \int d^3 \vec{y} d^3 \vec{z} \\
 &\times \int \left[\prod_{i=1}^8 \frac{d^3 \vec{k}_i}{(2\pi)^3} \right] e^{i\vec{y} \cdot (\vec{k}_1 + \vec{k}_2 + \vec{k}_3)} e^{i(\vec{x}_1 \cdot \vec{k}_4 + \vec{x}_2 \cdot \vec{k}_5)} e^{i\vec{z} \cdot (\vec{k}_6 + \vec{k}_7 + \vec{k}_8)} \\
 &\times \langle 0 | \hat{\zeta}_I(\vec{k}_4, \tau) \hat{\zeta}_I(\vec{k}_5, \tau) \hat{\zeta}_I(\vec{k}_1, \tau_1) \hat{\zeta}_I(\vec{k}_2, \tau_1) \hat{\zeta}_I(\vec{k}_3, \tau_1) \hat{\zeta}_I'(\vec{k}_6, \tau_2) \hat{\zeta}_I(\vec{k}_7, \tau_2) \hat{\zeta}_I(\vec{k}_8, \tau_2) | 0 \rangle.
 \end{aligned} \quad (52)$$

After Wick contractions, we find

$$\begin{aligned}
 \langle \hat{\zeta}(\vec{x}_1, \tau) \hat{\zeta}(\vec{x}_2, \tau) \rangle_{2\text{nd}}^{(0,2)} &= \int_{-\infty_-}^{\tau} d\tau_1 \epsilon(\tau_1) \epsilon'_2(\tau_1) a^2(\tau_1) \int_{-\infty_-}^{\tau_1} d\tau_2 \epsilon(\tau_2) \epsilon'_2(\tau_2) a^2(\tau_2) \int \frac{d^3 \vec{k}}{(2\pi)^3} \frac{d^3 \vec{q}}{(2\pi)^3} e^{i(\vec{x}_1 - \vec{x}_2) \cdot (\vec{k} + \vec{q})} \\
 &\times [\zeta_{k+q}^2(\tau) \{ \zeta_k(\tau_1) \zeta'_{k+q}(\tau_1) \zeta_q(\tau_1) \zeta_k^*(\tau_2) \zeta'_{k+q}(\tau_2) \zeta_q^*(\tau_2) \\
 &+ \zeta_k(\tau_1) \zeta'_{k+q}(\tau_1) \zeta_q(\tau_1) \zeta_{k+q}^*(\tau_2) [\zeta_k^*(\tau_2) \zeta_q^*(\tau_2) + \zeta_k^*(\tau_2) \zeta_q^*(\tau_2)] \\
 &+ \zeta_k^*(\tau_2) \zeta'_{k+q}(\tau_2) \zeta_q^*(\tau_2) \zeta_{k+q}(\tau_1) [\zeta_k'(\tau_1) \zeta_q(\tau_1) + \zeta_k(\tau_1) \zeta_q'(\tau_1)] \\
 &+ \zeta_k'(\tau_1) \zeta_{k+q}^*(\tau_1) \zeta_q(\tau_1) \zeta_{k+q}^*(\tau_2) [\zeta_q^*(\tau_2) \zeta_k^*(\tau_2) + \zeta_k^*(\tau_2) \zeta_q^*(\tau_2)] \\
 &+ \zeta_k^*(\tau_2) \zeta_{k+q}^*(\tau_2) \zeta_q^*(\tau_2) \zeta_{k+q}(\tau_1) [\zeta_q(\tau_1) \zeta_k'(\tau_1) + \zeta_k(\tau_1) \zeta_q'(\tau_1)] \}.
 \end{aligned} \quad (53)$$

At this point we shift the momentum following the prescription $k \rightarrow k - q$ in such a way that k is identified with the external momentum. The power spectrum at one loop can be therefore written as

$$\mathcal{P}(k) = \lim_{\tau \rightarrow 0^-} \left(\frac{k^3}{2\pi^2} \right) \left\{ |\zeta_k(\tau)|^2 + \frac{1}{(4\pi)^2} [\Delta P_1(k, \tau) + \Delta P_2(k, \tau)] \right\}, \quad (54)$$

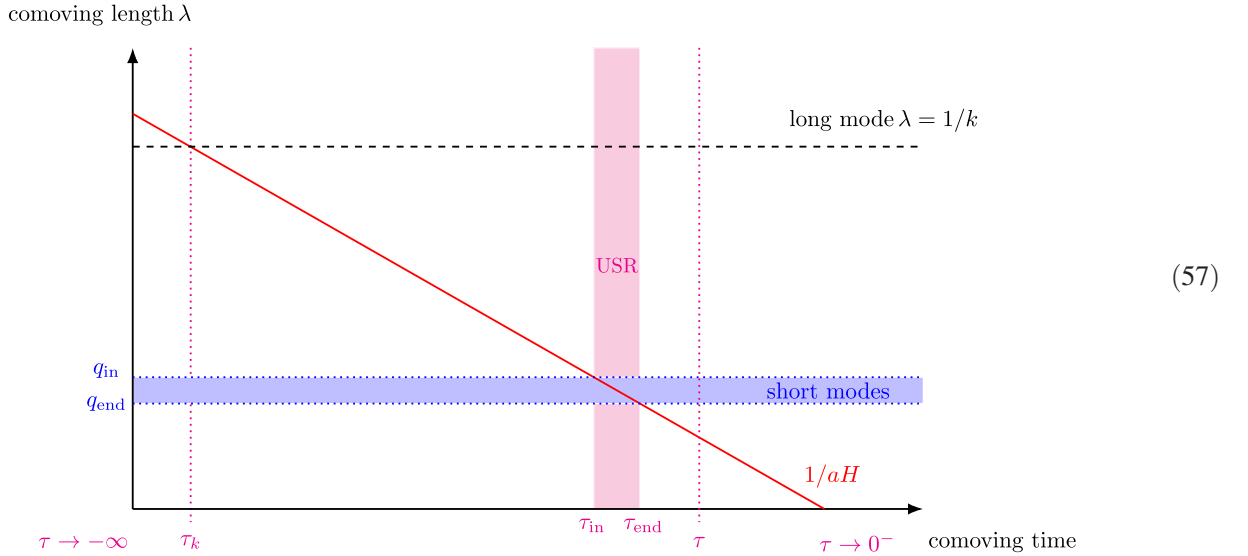
with

$$\begin{aligned}
 \Delta P_1(k, \tau) &\equiv 4 \int_{-\infty_+}^{\tau} d\tau_1 \epsilon(\tau_1) \epsilon'_2(\tau_1) a^2(\tau_1) \int_{-\infty_-}^{\tau} d\tau_2 \epsilon(\tau_2) \epsilon'_2(\tau_2) a^2(\tau_2) \int_0^{\infty} dq q^2 d(\cos \theta) |\zeta_k(\tau)|^2 \\
 &\times \{ \zeta_{k-q}(\tau_1) \zeta_k'(\tau_1) \zeta_q(\tau_1) \zeta_{k-q}^*(\tau_2) \zeta_k^*(\tau_2) \zeta_q^*(\tau_2) \\
 &+ \zeta_{k-q}(\tau_1) \zeta_k'(\tau_1) \zeta_q(\tau_1) \zeta_k^*(\tau_2) [\zeta_{k-q}^*(\tau_2) \zeta_q^*(\tau_2) + \zeta_{k-q}^*(\tau_2) \zeta_q^*(\tau_2)] \\
 &+ \zeta_{k-q}^*(\tau_2) \zeta_k^*(\tau_2) \zeta_q^*(\tau_2) \zeta_{k-q}(\tau_1) [\zeta_{k-q}'(\tau_1) \zeta_q(\tau_1) + \zeta_{k-q}(\tau_1) \zeta_q'(\tau_1)] \\
 &+ \zeta_{k-q}'(\tau_1) \zeta_k(\tau_1) \zeta_q(\tau_1) \zeta_k^*(\tau_2) [\zeta_q^*(\tau_2) \zeta_{k-q}^*(\tau_2) + \zeta_{k-q}^*(\tau_2) \zeta_q^*(\tau_2)] \\
 &+ \zeta_{k-q}^*(\tau_2) \zeta_k^*(\tau_2) \zeta_q^*(\tau_2) \zeta_{k-q}(\tau_1) [\zeta_q(\tau_1) \zeta_{k-q}'(\tau_1) + \zeta_{k-q}(\tau_1) \zeta_q'(\tau_1)] \},
 \end{aligned} \quad (55)$$

$$\begin{aligned}
\Delta P_2(k, \tau) \equiv & -8\text{Re} \left[\int_{-\infty}^{\tau} d\tau_1 \epsilon(\tau_1) \epsilon'_2(\tau_1) a^2(\tau_1) \int_{-\infty}^{\tau_1} d\tau_2 \epsilon(\tau_2) \epsilon'_2(\tau_2) a^2(\tau_2) \int_0^{\infty} dq q^2 d(\cos \theta) \zeta_k^2(\tau) \right. \\
& \times \{ \zeta_{k-q}(\tau_1) \zeta_k^{I*}(\tau_1) \zeta_q(\tau_1) \zeta_{k-q}^*(\tau_2) \zeta_k^{I*}(\tau_2) \zeta_q^*(\tau_2) \\
& + \zeta_{k-q}(\tau_1) \zeta_k^{I*}(\tau_1) \zeta_q(\tau_1) \zeta_k^*(\tau_2) [\zeta_{k-q}^{I*}(\tau_2) \zeta_q^*(\tau_2) + \zeta_{k-q}^*(\tau_2) \zeta_q^{I*}(\tau_2)] \\
& + \zeta_{k-q}^*(\tau_2) \zeta_k^{I*}(\tau_2) \zeta_q^*(\tau_2) \zeta_k^*(\tau_1) [\zeta_{k-q}^{I*}(\tau_1) \zeta_q(\tau_1) + \zeta_{k-q}^*(\tau_1) \zeta_q^{I*}(\tau_1)] \\
& + \zeta_{k-q}^{I*}(\tau_1) \zeta_k^*(\tau_1) \zeta_q(\tau_1) \zeta_k^*(\tau_2) [\zeta_q^*(\tau_2) \zeta_{k-q}^{I*}(\tau_2) + \zeta_{k-q}^*(\tau_2) \zeta_q^{I*}(\tau_2)] \\
& \left. + \zeta_{k-q}^{I*}(\tau_2) \zeta_k^*(\tau_2) \zeta_q^*(\tau_2) \zeta_k^*(\tau_1) [\zeta_q(\tau_1) \zeta_{k-q}^{I*}(\tau_1) + \zeta_{k-q}^*(\tau_1) \zeta_q^{I*}(\tau_1)] \right\}. \quad (56)
\end{aligned}$$

A. Loop correction with a large hierarchy of scales

First, we will be concerned with external momenta that describe the large CMB scales, while the USR takes place when modes $k_{\text{USR}} \gg k$ cross the horizon. The situation is summarized in the following schematic



in which the blue horizontal band represents the interval of modes that cross the horizon during the USR phase, the vertical band shaded in magenta. In other words, as we will restrict the integration over momenta $q \in [q_{\text{in}}, q_{\text{end}}]$ that are enhanced by the USR phase, we can assume $q \gg k$. Consequently, as in Ref. [35], we approximate

$$k - q = \sqrt{k^2 + q^2 - 2kq \cos(\theta)} \approx q, \quad \int_{-1}^{+1} d(\cos \theta) = 2. \quad (58)$$

With these assumptions, we can further simplify the expressions. We collect each contribution depending on the number of time derivatives acting on the long mode ζ_k . In each expression, the first line indicates terms with no derivative on the long modes, the second one those with one derivative, while the last with two. One finds

$$\begin{aligned}
\Delta P_1(k, \tau) \equiv & 8 \int_{\tau_{\text{in}}}^{\tau} d\tau_1 \epsilon(\tau_1) \epsilon'_2(\tau_1) a^2(\tau_1) \int_{\tau_{\text{in}}}^{\tau} d\tau_2 \epsilon(\tau_2) \epsilon'_2(\tau_2) a^2(\tau_2) \int_{q_{\text{in}}}^{q_{\text{end}}} dq q^2 |\zeta_k(\tau)|^2 \\
& \times \{ 4\zeta_k(\tau_1) \zeta_k^*(\tau_2) \zeta_q(\tau_1) \zeta_q^*(\tau_2) \zeta_q^{I*}(\tau_2) \zeta_q^*(\tau_2) \\
& + 2\zeta_k^{I*}(\tau_1) \zeta_k^*(\tau_2) \zeta_q(\tau_1) \zeta_q^*(\tau_2) \zeta_q^{I*}(\tau_2) \zeta_q^*(\tau_2) + 2\zeta_k(\tau_1) \zeta_k^{I*}(\tau_2) \zeta_q(\tau_1) \zeta_q^*(\tau_2) \zeta_q^{I*}(\tau_2) \zeta_q^*(\tau_2) \\
& + \zeta_k^{I*}(\tau_1) \zeta_k^*(\tau_2) \zeta_q(\tau_1) \zeta_q^*(\tau_2) \zeta_q^{I*}(\tau_2) \zeta_q^*(\tau_2) \}, \quad (59)
\end{aligned}$$

$$\begin{aligned} \Delta P_2(k, \tau) \equiv & -16\text{Re} \left[\int_{\tau_{\text{in}}}^{\tau} d\tau_1 \epsilon(\tau_1) \epsilon'_2(\tau_1) a^2(\tau_1) \int_{\tau_{\text{in}}}^{\tau_1} d\tau_2 \epsilon(\tau_2) \epsilon'_2(\tau_2) a^2(\tau_2) \int_{q_{\text{in}}}^{q_{\text{end}}} dq q^2 \zeta_k(\tau)^2 \right. \\ & \times \{ 4\zeta_k^*(\tau_1) \zeta_k^*(\tau_2) \zeta'_q(\tau_1) \zeta_q(\tau_1) \zeta_q^*(\tau_2) \zeta'_q(\tau_2) + 2\zeta_k^{\prime*}(\tau_1) \zeta_k^*(\tau_2) \zeta_q(\tau_1)^2 \zeta_q^{\prime*}(\tau_2) \zeta_q^*(\tau_2) \\ & \left. + 2\zeta_k^*(\tau_1) \zeta_k^{\prime*}(\tau_2) \zeta'_q(\tau_1) \zeta_q(\tau_1) \zeta_q^*(\tau_2)^2 + \zeta_k^*(\tau_1) \zeta_k^{\prime*}(\tau_2) \zeta_q(\tau_1)^2 \zeta_q^*(\tau_2)^2 \} \right]. \end{aligned} \quad (60)$$

We can combine the two contributions using the properties of symmetric integrals for holomorphic symmetric functions $f(\tau_1, \tau_2) = f(\tau_2, \tau_1)$ [60]

$$\int_{\tau_{\text{in}}}^{\tau} d\tau_1 \int_{\tau_{\text{in}}}^{\tau_1} d\tau_2 f(\tau_1, \tau_2) = \frac{1}{2} \int_{\tau_{\text{in}}}^{\tau} d\tau_1 \int_{\tau_{\text{in}}}^{\tau} d\tau_2 f(\tau_1, \tau_2). \quad (61)$$

To shorten the notation, we introduce $\Delta P(k, \tau) = \Delta P_1(k, \tau) + \Delta P_2(k, \tau)$ and collect the individual contribution order by order in derivatives:

- (1) Zeroth order in time derivatives of the long mode. For ease of reading, we introduce the short-hand notation $\epsilon(\tau) \epsilon'_2(\tau) a^2(\tau) \equiv g(\tau)$. Consider the sum of the two integrals

$$\Delta P_{0\text{th}}(k, \tau) = 32 \int_{\tau_{\text{in}}}^{\tau} d\tau_1 g(\tau_1) \int_{\tau_{\text{in}}}^{\tau} d\tau_2 g(\tau_2) \int_{q_{\text{in}}}^{q_{\text{end}}} dq q^2 |\zeta_k(\tau)|^2 \zeta_k(\tau_1) \zeta_k^*(\tau_2) \zeta_q(\tau_1) \zeta'_q(\tau_1) \zeta_q^*(\tau_2) \zeta_q^{\prime*}(\tau_2) \quad (62)$$

$$- 64\text{Re} \left[\int_{\tau_{\text{in}}}^{\tau} d\tau_1 g(\tau_1) \int_{\tau_{\text{in}}}^{\tau_1} d\tau_2 g(\tau_2) \int_{q_{\text{in}}}^{q_{\text{end}}} dq q^2 \zeta_k(\tau)^2 \zeta_k^*(\tau_1) \zeta_k^*(\tau_2) \zeta'_q(\tau_1) \zeta_q(\tau_1) \zeta_q^*(\tau_2) \zeta_q^{\prime*}(\tau_2) \right]. \quad (63)$$

We notice that, in the first integral in Eq. (62), the exchange $\tau_1 \leftrightarrow \tau_2$ transforms

$$\begin{aligned} \zeta_k(\tau_1) \zeta_k^*(\tau_2) \zeta_q(\tau_1) \zeta'_q(\tau_1) \zeta_q^*(\tau_2) \zeta_q^{\prime*}(\tau_2) & \xrightarrow{\tau_1 \leftrightarrow \tau_2} \zeta_k(\tau_2) \zeta_k^*(\tau_1) \zeta_q(\tau_2) \zeta'_q(\tau_2) \zeta_q^*(\tau_1) \zeta_q^{\prime*}(\tau_1) \\ & = [\zeta_k(\tau_1) \zeta_k^*(\tau_2) \zeta_q(\tau_1) \zeta'_q(\tau_1) \zeta_q^*(\tau_2) \zeta_q^{\prime*}(\tau_2)]^*. \end{aligned} \quad (64)$$

Therefore, the first integral in Eq. (62) is fully symmetric under the exchange $\tau_1 \leftrightarrow \tau_2$, and we rewrite $\Delta P_{0\text{th}}(k, \tau)$ as

$$\Delta P_{0\text{th}}(k, \tau) = 32 \int_{\tau_{\text{in}}}^{\tau} d\tau_1 g(\tau_1) \int_{\tau_{\text{in}}}^{\tau} d\tau_2 g(\tau_2) \int_{q_{\text{in}}}^{q_{\text{end}}} dq q^2 |\zeta_k(\tau)|^2 \text{Re}[\zeta_k(\tau_1) \zeta_k^*(\tau_2) \zeta_q(\tau_1) \zeta'_q(\tau_1) \zeta_q^*(\tau_2) \zeta_q^{\prime*}(\tau_2)] \quad (65)$$

$$- 64 \int_{\tau_{\text{in}}}^{\tau} d\tau_1 g(\tau_1) \int_{\tau_{\text{in}}}^{\tau_1} d\tau_2 g(\tau_2) \int_{q_{\text{in}}}^{q_{\text{end}}} dq q^2 \text{Re}[\zeta_k(\tau)^2 \zeta_k^*(\tau_1) \zeta_k^*(\tau_2) \zeta'_q(\tau_1) \zeta_q(\tau_1) \zeta_q^*(\tau_2) \zeta_q^{\prime*}(\tau_2)]. \quad (66)$$

and apply to the first integral in Eq. (65) the identity in Eq. (61). We arrive at

$$\begin{aligned} \Delta P_{0\text{th}}(k, \tau) = & 64 \int_{\tau_{\text{in}}}^{\tau} d\tau_1 g(\tau_1) \int_{\tau_{\text{in}}}^{\tau_1} d\tau_2 g(\tau_2) \int_{q_{\text{in}}}^{q_{\text{end}}} dq q^2 \{ \text{Re}[\zeta_k(\tau) \zeta_k^*(\tau) \zeta_k(\tau_1) \zeta_k^*(\tau_2) \zeta_q(\tau_1) \zeta'_q(\tau_1) \zeta_q^*(\tau_2) \zeta_q^{\prime*}(\tau_2)] \\ & - \text{Re}[\zeta_k(\tau)^2 \zeta_k^*(\tau_1) \zeta_k^*(\tau_2) \zeta'_q(\tau_1) \zeta_q(\tau_1) \zeta_q^*(\tau_2) \zeta_q^{\prime*}(\tau_2)] \}. \end{aligned} \quad (67)$$

We are now in the position of combining the two integrand functions. Schematically, we define the two combinations

$$X \equiv \zeta_k^*(\tau) \zeta_k(\tau_1), \quad Y \equiv \zeta_k(\tau) \zeta_q(\tau_1) \zeta'_q(\tau_1) \zeta_k^*(\tau_2) \zeta_q^*(\tau_2) \zeta_q^{\prime*}(\tau_2), \quad (68)$$

such that the integrand in Eq. (67) becomes

$$\text{Re}(XY) - \text{Re}(X^*Y) = -2\text{Im}(X)\text{Im}(Y). \quad (69)$$

We thus arrive at the result

Contribution with no time derivatives on the long mode k

$$\Delta P_{0th}(k, \tau) = -128 \int_{\tau_{in}}^{\tau} d\tau_1 \epsilon(\tau_1) \epsilon'_2(\tau_1) a^2(\tau_1) \int_{\tau_{in}}^{\tau_1} d\tau_2 \epsilon(\tau_2) \epsilon'_2(\tau_2) a^2(\tau_2) \int_{q_{in}}^{q_{end}} dq q^2 \times \text{Im}[\zeta_k^*(\tau) \zeta_k(\tau_1)] \text{Im}[\zeta_k(\tau) \zeta_q(\tau_1) \zeta'_q(\tau_1) \zeta_k^*(\tau_2) \zeta_q^*(\tau_2) \zeta'_q(\tau_2)]. \quad (70)$$

Given that we are interested in modes k that are much smaller than the USR-enhanced ones, they are superhorizon at the time of USR phase. Thus, for any time $\tau \gtrsim \tau_{in}$ of relevance for both time integrations, one has that

$$\text{Im}[\zeta_k(\tau) \zeta_k^*(\tau_1)] \simeq \text{Im}[|\zeta_k(\tau)|^2] = 0, \quad (71)$$

which makes the above contribution negligible.

- (2) First order in time derivatives of the long mode. Starting from the second lines of Eqs. (59), (60), we now consider the sum

$$\begin{aligned} \Delta P_{1st}(k, \tau) = & 16 \int_{\tau_{in}}^{\tau} d\tau_1 g(\tau_1) \int_{\tau_{in}}^{\tau} d\tau_2 g(\tau_2) \int_{q_{in}}^{q_{end}} dq q^2 |\zeta_k(\tau)|^2 \\ & \times [\zeta'_k(\tau_1) \zeta_k^*(\tau_2) \zeta_q(\tau_1) \zeta_q(\tau_2) \zeta'_q(\tau_2) \zeta_q^*(\tau_2) + \zeta_k(\tau_1) \zeta_k'^*(\tau_2) \zeta_q(\tau_1) \zeta'_q(\tau_1) \zeta_q^*(\tau_2) \zeta_q^*(\tau_2)] \\ & - 32 \text{Re} \left\{ \int_{\tau_{in}}^{\tau} d\tau_1 g(\tau_1) \int_{\tau_{in}}^{\tau_1} d\tau_2 g(\tau_2) \int_{q_{in}}^{q_{end}} dq q^2 \zeta_k(\tau)^2 \right. \\ & \times [\zeta_k'^*(\tau_1) \zeta_k^*(\tau_2) \zeta_q(\tau_1)^2 \zeta_q'^*(\tau_2) \zeta_q^*(\tau_2) + \zeta_k^*(\tau_1) \zeta_k'^*(\tau_2) \zeta_q(\tau_1) \zeta_q(\tau_2) \zeta_q^*(\tau_2)^2] \left. \right\}. \quad (72) \end{aligned}$$

Manipulations analog to those discussed in the previous point allow one to combine the two integrals together. We find

$$\begin{aligned} \Delta P_{1st}(k, \tau) = & -64 \int_{\tau_{in}}^{\tau} d\tau_1 g(\tau_1) \int_{\tau_{in}}^{\tau_1} d\tau_2 g(\tau_2) \int_{q_{in}}^{q_{end}} dq q^2 \{ \text{Im}[\zeta_k^*(\tau) \zeta_k(\tau_1)] \text{Im}[\zeta_k(\tau) \zeta_k^*(\tau_2)^2 \zeta_q(\tau_1) \zeta_k'^*(\tau_2) \zeta'_q(\tau_1)] \\ & + \text{Im}[\zeta_k^*(\tau) \zeta'_k(\tau_1)] \text{Im}[\zeta_k(\tau) \zeta_q(\tau_1)^2 \zeta_k^*(\tau_2) \zeta_q^*(\tau_2) \zeta_q'^*(\tau_2)] \}. \quad (73) \end{aligned}$$

Again, since we are interested in modes k that are much smaller than the USR-enhanced ones, and are superhorizon at the time of USR phase, the contribution within the curly brackets in the first line vanishes thanks to Eq. (71). This leaves us with

Contribution with one time derivatives on the long mode k

$$\begin{aligned} \Delta P_{1st}(k, \tau) \equiv & -64 \int_{\tau_{in}}^{\tau} d\tau_1 \epsilon(\tau_1) \epsilon'_2(\tau_1) a^2(\tau_1) \int_{\tau_{in}}^{\tau_1} d\tau_2 \epsilon(\tau_2) \epsilon'_2(\tau_2) a^2(\tau_2) \int_{q_{in}}^{q_{end}} dq q^2 \\ & \times \text{Im}[\zeta_k^*(\tau) \zeta'_k(\tau_1)] \text{Im}[\zeta_k(\tau) \zeta_q(\tau_1) \zeta_q(\tau_1) \zeta_k^*(\tau_2) \zeta_q^*(\tau_2) \zeta'_q(\tau_2)]. \quad (74) \end{aligned}$$

- (3) Second order in time derivatives of the long mode. Analog manipulations give

Contribution with two time derivatives on the long mode k

$$\begin{aligned} \Delta P_{2nd}(k, \tau) \equiv & -32 \int_{\tau_{in}}^{\tau} d\tau_1 \epsilon(\tau_1) \epsilon'_2(\tau_1) a^2(\tau_1) \int_{\tau_{in}}^{\tau_1} d\tau_2 \epsilon(\tau_2) \epsilon'_2(\tau_2) a^2(\tau_2) \int_{q_{in}}^{q_{end}} dq q^2 \\ & \times \text{Im}[\zeta_k^*(\tau) \zeta'_k(\tau_1)] \text{Im}[\zeta_k(\tau) \zeta_q(\tau_1) \zeta_q(\tau_1) \zeta_k^*(\tau_2) \zeta_q^*(\tau_2) \zeta_q^*(\tau_2)]. \quad (75) \end{aligned}$$

We stress that the only approximation employed so far is to take the external momentum to be much smaller than the one in the loop, i.e., $k \ll q$, which is justified in presence of a large hierarchy between the CMB and the USR scales.

B. Loop correction at any scales

It will be useful in the following to remove the assumption that the external momentum is much smaller than the modes in the loop, i.e., the large separation of scales $k \ll q$. Starting again from Eqs. (54), (55), (56), we can proceed with analogous steps as in the previous section and define

$$\begin{aligned}
X_1 &\equiv \zeta_k^*(\tau) \zeta'_k(\tau_1), & Y_1 &\equiv \zeta_k(\tau) \zeta_{k-q}(\tau_1) \zeta_q(\tau_1) \zeta_{k-q}^*(\tau_2) \zeta'_k(\tau_2) \zeta_q^*(\tau_2), \\
X_2 &\equiv \zeta_k^*(\tau) \zeta'_k(\tau_1), & Y_2 &\equiv \zeta_k(\tau) \zeta_{k-q}(\tau_1) \zeta_q(\tau_1) \zeta_k^*(\tau_2) [\zeta_{k-q}'^*(\tau_2) \zeta_q^*(\tau_2) + \zeta_{k-q}^*(\tau_2) \zeta_q'^*(\tau_2)], \\
X_3 &\equiv \zeta_k^*(\tau) \zeta_k(\tau_1), & Y_3 &\equiv \zeta_k(\tau) \zeta_{k-q}^*(\tau_2) \zeta_q'^*(\tau_2) \zeta_q^*(\tau_2) [\zeta_{k-q}'(\tau_1) \zeta_q(\tau_1) + \zeta_{k-q}(\tau_1) \zeta_q'(\tau_1)] \\
X_4 &\equiv \zeta_k^*(\tau) \zeta_k(\tau_1), & Y_4 &\equiv \zeta_k(\tau) \zeta_{k-q}'(\tau_1) \zeta_q(\tau_1) \zeta_k^*(\tau_2) [\zeta_q^*(\tau_2) \zeta_{k-q}'^*(\tau_2) + \zeta_{k-q}^*(\tau_2) \zeta_q'^*(\tau_2)] \\
X_5 &\equiv \zeta_k^*(\tau) \zeta_k(\tau_1), & Y_5 &\equiv \zeta_k(\tau) \zeta_{k-q}'^*(\tau_2) \zeta_k^*(\tau_2) \zeta_q^*(\tau_2) [\zeta_q(\tau_1) \zeta_{k-q}'(\tau_1) + \zeta_{k-q}(\tau_1) \zeta_q'(\tau_1)]
\end{aligned} \tag{76}$$

in such a way that $\Delta P \equiv \Delta P_1 + \Delta P_2$ can be written in the schematic form

Generic loop correction at any scale k

$$\Delta P(k, \tau) \equiv -16 \int_{\tau_{\text{in}}}^{\tau} d\tau_1 g(\tau_1) \int_{\tau_{\text{in}}}^{\tau_1} d\tau_2 g(\tau_2) \int_{q_{\text{in}}}^{q_{\text{end}}} dq q^2 \int_{-1}^1 d(\cos \theta) \times \sum_{i=1}^5 \text{Im}(X_i) \text{Im}(Y_i), \tag{77}$$

thanks to the identity in Eq. (69) and where we again introduced $\epsilon(\tau) \epsilon'_2(\tau) a^2(\tau) \equiv g(\tau)$. This expression is much more intricate than the one obtained in the limit of a large hierarchy of scales between the mode k and the USR loop momenta. It will allow us to seize the loop correction to the power spectrum also at the USR scales where the peak of the power spectrum is generated.

IV. TIME INTEGRATION BEYOND THE INSTANTANEOUS TRANSITION AND AT ANY SCALES

A. Loop evaluation at the CMB scales

Let us try to simplify the structure of Eq. (54) in light of the approximations introduced so far. First of all, let us write Eq. (54) in the form

$$\begin{aligned}
\mathcal{P}(k) &= \frac{H^2}{8\pi^2 \epsilon_{\text{ref}}} \left\{ 1 + \lim_{\tau \rightarrow 0^-} \frac{4\epsilon_{\text{ref}} k^3}{H^2 (4\pi)^2} \Delta P_{1\text{st}}(k, \tau) \right. \\
&\quad \left. + \lim_{\tau \rightarrow 0^-} \frac{4\epsilon_{\text{ref}} k^3}{H^2 (4\pi)^2} \Delta P_{2\text{nd}}(k, \tau) \right\}, \tag{78}
\end{aligned}$$

where we used the slow-roll approximation for the first term in Eq. (54) given that k is of the order of the CMB pivot scale. We focus on the leading correction given by $\Delta P_{1\text{st}}(k, \tau)$. Using the number of e -folds as the time variable, we find that it can be written in the compact form [cf. our definition in Eq. (1)]

$$\begin{aligned}
\Delta \mathcal{P}_{1\text{-loop}}(k_*) &\equiv \lim_{\tau \rightarrow 0^-} \frac{4\epsilon_{\text{ref}} k^3}{H^2 (4\pi)^2} \Delta P_{1\text{st}}(k, \tau) \\
&= 32 \left(\frac{H^2}{8\pi^2 \epsilon_{\text{ref}}} \right) \int_{N_{\text{in}} - \Delta N}^{N_{\text{end}} + \Delta N} dN_1 \frac{d\eta}{dN}(N_1) \\
&\quad \times \int_{N_{\text{in}} - \Delta N}^{N_1} dN_2 \bar{\epsilon}(N_2) \frac{d\eta}{dN}(N_2) e^{3(N_2 - N_{\text{in}})} \\
&\quad \times \int \frac{d\bar{q}}{\bar{q}^4} \text{Im} \left[\bar{\zeta}_q(N_1)^2 \bar{\zeta}_q^*(N_2) \frac{d\bar{\zeta}_q^*}{dN}(N_2) \right], \tag{79}
\end{aligned}$$

where we introduced the following manipulations:

- (i) We use the approximation $\epsilon_2(N) \approx -2\eta(N)$. This is because in the relevant range of N over which we integrate $\epsilon \ll 1$ while $\eta = O(1)$, cf. the right panel of Fig. 2.
- (ii) We define $\bar{q} \equiv q/a_{\text{in}}H$. Furthermore, we use the two relations

$$\begin{aligned}
\frac{a(N_1)H}{k} &= e^{N_1 - N_k}, \quad \text{with } a(N_k)H = k, \quad \text{and} \\
\frac{a(N_2)H}{q} &= \frac{e^{N_2 - N_{\text{in}}}}{\bar{q}}. \tag{80}
\end{aligned}$$

- (iii) We introduce the short-hand notation

$$\bar{\zeta}_q(N) \equiv \frac{\epsilon_{\text{ref}}^{1/2} q^{3/2} \zeta_q(N)}{H}. \tag{81}$$

The virtue of this definition is that $\bar{\zeta}_q(N)$ is precisely the quantity we compute numerically by solving the M-S equation, cf. the right panel of Fig. 3. Furthermore, it should be noted that the definition in Eq. (81) is automatically invariant under the rescaling in Eq. (10). The same comment applies to the definition of \bar{q} and the ratios in Eq. (80). Consequently, an expression entirely written in terms of barred quantities is automatically invariant under the rescaling in Eq. (10).

- (iv) Importantly, in the derivation of Eq. (79) we use (cf. Appendix)

$$\begin{aligned}
\text{Im} \left[\bar{\zeta}_k^*(N) \frac{d\bar{\zeta}_k}{dN}(N_1) \right] &\simeq \text{Im} \left[\bar{\zeta}_k^*(N_1) \frac{d\bar{\zeta}_k}{dN}(N_1) \right] \\
&= -\frac{\bar{k}^3}{4\bar{\epsilon}(N_1)} e^{3(N_{\text{in}} - N_1)}, \tag{82}
\end{aligned}$$

with $\epsilon(N)$ given by Eq. (32) for generic δN . This is because $N_{1,2}$ vary at around N_{end} , and in this time interval modes with comoving wave numbers $k \approx k_*$ are way outside the horizon and stay constant.

For the very same reason, we also use the slow-roll approximation

$$\bar{\zeta}_k(N_1)\bar{\zeta}_k^*(N_2) = \frac{1}{4}. \quad (83)$$

- (v) The range of integration in Eq. (79) is as follows. In the case of a smooth transition, we take $N_1 \in [N_{\text{in}} - \Delta N, N_{\text{end}} + \Delta N]$ and $N_2 \in [N_{\text{in}} - \Delta N, N_1]$, where ΔN should be large enough to complete the SR/USR/SR transition (that is, $\Delta N \gtrsim \delta N$). In the limit of instantaneous transition, we set $N_1 = N_2 = N_{\text{end}}$,

which corresponds to consider the dominant contribution given by the first δ function in Eq. (31). Moreover, we include a factor 1/2 since, with respect to the integration over N_2 , the argument of the δ function in Eq. (31) picks up the upper limit of the integration interval at N_{end} . The integration over q , on the contrary, is limited by $\bar{q} \in [1, e^{\Delta N_{\text{USR}}}]$.

1. The instantaneous transition

We consider the instantaneous limit (dubbed $\delta N \rightarrow 0$ in the following) of Eq. (79). We find

$$\lim_{\delta N \rightarrow 0} \Delta \mathcal{P}_{1\text{-loop}}(k_*) = \left(\frac{H^2}{8\pi^2 \epsilon_{\text{ref}}} \right) \eta_{\text{II}}^2 \left(\frac{k_{\text{end}}}{k_{\text{in}}} \right)^{-2\eta_{\text{II}}+3} \lim_{\delta N \rightarrow 0} (16) \int_1^{e^{\Delta N_{\text{USR}}}} \frac{d\bar{q}}{\bar{q}^4} |\bar{\zeta}_q(N_{\text{end}})|^2 \text{Im} \left[\bar{\zeta}_q(N_{\text{end}}) \frac{d\bar{\zeta}_q^*}{dN}(N_{\text{end}}) \right]. \quad (84)$$

This expression can be further simplified using [cf. Eq. (A12)]

$$\text{Im} \left[\bar{\zeta}_q(N_{\text{end}}) \frac{d\bar{\zeta}_q^*}{dN}(N_{\text{end}}) \right] = \frac{\bar{q}^3}{4} e^{(2\eta_{\text{II}}-3)(N_{\text{end}}-N_{\text{in}})} = \frac{\bar{q}^3}{4} \left(\frac{k_{\text{end}}}{k_{\text{in}}} \right)^{2\eta_{\text{II}}-3}, \quad (85)$$

so that we write

$$\lim_{\delta N \rightarrow 0} \Delta \mathcal{P}_{1\text{-loop}}(k_*) = \left(\frac{H^2}{8\pi^2 \epsilon_{\text{ref}}} \right) 4\eta_{\text{II}}^2 \lim_{\delta N \rightarrow 0} \int_1^{e^{\Delta N_{\text{USR}}}} \frac{d\bar{q}}{\bar{q}} |\bar{\zeta}_q(N_{\text{end}})|^2. \quad (86)$$

We remark that this expression is valid for generic values of η_{II} during USR.

We consider now the computation of the last integral. The factor $\bar{\zeta}_q$ grows exponentially during the USR phase. In the case of subhorizon modes, we have $\bar{\zeta}_q(N) \sim e^{-(1-\eta_{\text{II}})N}$, while in the case of superhorizon modes we find $\bar{\zeta}_q(N) \sim e^{-(3-2\eta_{\text{II}})N}$ (cf. Appendix). However, the precise estimate of the integral in Eq. (86) is complicated by the fact that curvature modes $\bar{\zeta}_q$ with $\bar{q} \in [1, \exp(\Delta N_{\text{USR}})]$ are neither sub- nor superhorizon but they exit the horizon during the USR phase, thus making the analytical estimate of the argument of their exponential growth more challenging.

The situation simplifies if we consider some special values of η_{II} . We consider the case $\eta_{\text{II}} = 3$ (that is $\epsilon_2 = -6$,

it should be noted that this is also the case studied in Ref. [35]). In this case, everything can be computed analytically. We find the scaling

$$\begin{aligned} \lim_{\delta N \rightarrow 0} \int_1^{e^{\Delta N_{\text{USR}}}} \frac{d\bar{q}}{\bar{q}} |\bar{\zeta}_q(N_{\text{end}})|^2 &\approx \frac{e^{6\Delta N_{\text{USR}}}}{4} (1 + \Delta N_{\text{USR}}) \\ &= \frac{1}{4} \left(\frac{k_{\text{end}}}{k_{\text{in}}} \right)^6 \left[1 + \log \left(\frac{k_{\text{end}}}{k_{\text{in}}} \right) \right], \end{aligned} \quad (87)$$

which becomes more and more accurate for larger $k_{\text{end}}/k_{\text{in}}$. The final result is

Leading one-loop correction at CMB scales in the instantaneous SR/USR/SR transition

$$\lim_{\delta N \rightarrow 0} \Delta \mathcal{P}_{1\text{-loop}}(k_*) \approx \left(\frac{H^2}{8\pi^2 \epsilon_{\text{ref}}} \right) \eta_{\text{II}}^2 \left(\frac{k_{\text{end}}}{k_{\text{in}}} \right)^6 \left[1 + \log \left(\frac{k_{\text{end}}}{k_{\text{in}}} \right) \right], \quad \text{with } \eta_{\text{II}} = 3, \eta_{\text{III}} = 0 \quad (88)$$

which perfectly agrees with the findings of Ref. [35] in the same limit.

The above result has a number of limitations, which we address separately in the following subsections:

- (1) Dynamics during USR, Sec. IV A 2. We modify the assumption $\eta_{\text{II}}=3$ and we take $\delta N \rightarrow 0$ and $\eta_{\text{III}} = 0$.
- (2) Dynamics at the SR/USR/SR transition, Sec. IV A 3. We consider $\delta N \neq 0$, with generic η_{II} but $\eta_{\text{III}} = 0$.

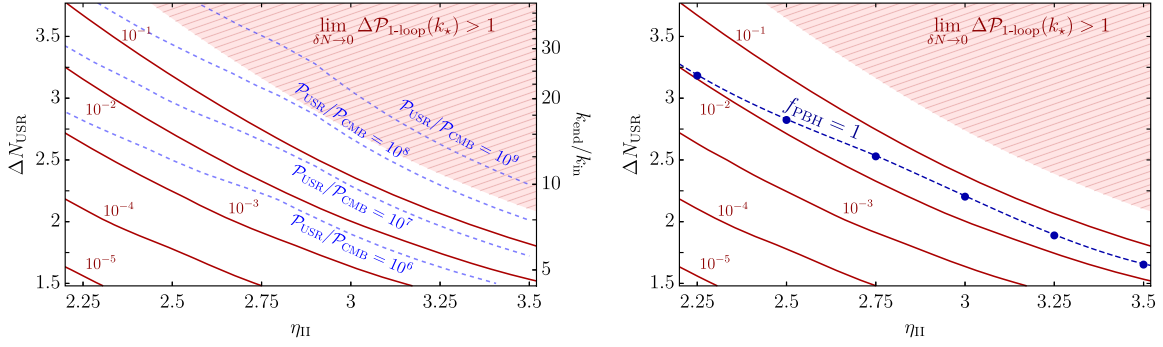


FIG. 4. In both panels, we consider a generic USR dynamics with varying η_{II} (x axis) and ΔN_{USR} (y axis). We take $\eta_{\text{III}} = 0$ and the instantaneous limit $\delta N = 0$. We plot in solid red contours of constant $\lim_{\delta N \rightarrow 0} \Delta \mathcal{P}_{1\text{-loop}}(k_*)$, defined in Eq. (79) and computed according to Eq. (86) with $H^2/8\pi^2\epsilon_{\text{ref}} = 2.1 \times 10^{-9}$. The region hatched in red is defined by the condition $\lim_{\delta N \rightarrow 0} \Delta \mathcal{P}_{1\text{-loop}}(k_*) > 1$. Left panel: we superimpose contours of constant $\mathcal{P}_{\text{USR}}/\mathcal{P}_{\text{CMB}}$ as defined in Eq. (89) (dashed blue). Right panel: we superimpose the line defined by the condition $f_{\text{PBH}} = 1$. Along this line, we get 100% of DM in the form of asteroid-mass PBHs.

Considering a nonzero value of δN is very important because it corresponds to a more realistic smooth SR/USR/SR transition, as opposed to the instantaneous limit with $\delta N = 0$.

2. Dynamics during USR

We compute Eq. (86) for generic values of η_{II} , still keeping $\delta N \rightarrow 0$ and $\eta_{\text{III}} = 0$. From the computation of the tree-level power spectrum (cf. Sec. II B and Fig. 3) we define

$$\frac{\mathcal{P}_{\text{USR}}}{\mathcal{P}_{\text{CMB}}} \equiv \frac{\mathcal{P}(\bar{k}_{\text{max}})}{\mathcal{P}(\bar{k} \ll 1)}, \quad (89)$$

where \bar{k}_{max} represents the position of the max of $\mathcal{P}(\bar{k})$ after the growth due to the USR dynamics. We compare in the left panel of Fig. 4 contours of constant $\mathcal{P}_{\text{USR}}/\mathcal{P}_{\text{CMB}}$ (dashed blue) and constant $\lim_{\delta N \rightarrow 0} \Delta \mathcal{P}_{1\text{-loop}}(k_*)$ (solid red). We take $H^2/8\pi^2\epsilon_{\text{ref}} = 2.1 \times 10^{-9}$. Our analysis shows that enhancements $\mathcal{P}_{\text{USR}}/\mathcal{P}_{\text{CMB}} \gtrsim 10^8$ are barely compatible with the perturbativity condition $\lim_{\delta N \rightarrow 0} \Delta \mathcal{P}_{1\text{-loop}}(k_*) < 1$, which roughly means “loops < tree level.” The region $\lim_{\delta N \rightarrow 0} \Delta \mathcal{P}_{1\text{-loop}}(k_*) > 1$ is hatched in red in Fig. 4.

We can actually do better and compare with a careful computation of the PBH abundance. The parameters of the dynamics in Sec. II B (with $\eta_{\text{III}} = 0$ and $\delta N \rightarrow 0$) are chosen in such a way that the integral

$$f_{\text{PBH}} \equiv \frac{\Omega_{\text{PBH}}}{\Omega_{\text{CDM}}} = \int f_{\text{PBH}}(M_{\text{PBH}}) d \log M_{\text{PBH}} \approx 1, \quad (90)$$

which means that we get $\approx 100\%$ of DM in the form of PBHs. More in detail, we tune, for each η_{II} , the value of ΔN_{USR} so to get $f_{\text{PBH}} \approx 1$; we choose the numerical value of k_{in} in such a way that the peak of the PBH mass distribution $f_{\text{PBH}}(M_{\text{PBH}})$ falls within the interval

$M_{\text{PBH}}/M_{\odot} \in [10^{-14}, 10^{-13}]$ in which the condition $f_{\text{PBH}} \approx 1$ is experimentally allowed, the so-called asteroid-mass PBHs [10]. We compute Eq. (90) using threshold statistics and including the full nonlinear relation between the curvature and the density contrast fields (cf. [61,62]). The interested reader can find more details on the computation of the abundance in Ref. [54] and references therein.³ In the right panel of Fig. 4 we plot the line defined by the condition $f_{\text{PBH}} \approx 1$. The comparison between the left- and right-hand side of Fig. 4 shows that, in order to fulfil the condition $f_{\text{PBH}} \approx 1$, one needs $\mathcal{P}_{\text{USR}}/\mathcal{P}_{\text{CMB}} = O(10^7)$.⁴

We conclude that the condition $f_{\text{PBH}} \approx 1$ lies within the region in which perturbativity is still applicable. This is in contrast with the conclusion reached in Refs. [35,37,39] in the limit of instantaneous SR/USR/SR transition. The origin of the difference is the more accurate calculation of the PBHs abundance performed in our work. In particular, in previous analyses, estimates of $f_{\text{PBH}} \approx 1$ are based on requiring $\mathcal{P}_{\text{USR}} \simeq 10^{-2}$, and on the scaling $\Delta \mathcal{P} = (k_{\text{end}}/k_{\text{in}})^{2\eta_{\text{II}}}$ in order to capture the growth of the power spectrum at small scales. However, as explained in Sec. II B, this scaling does not accurately describe the amplitude of the power spectrum at its peak, see the left

³It is possible to further improve our analysis by including the presence of primordial non-Gaussianity (e.g., [63–71]). In the case of local non-Gaussianity parametrized by a positive non-Gaussian parameter f_{NL} , as expected in the case of USR, we generically expect a larger abundance of PBHs compared to the Gaussian case [72–76]. This means that, in order to achieve the same abundance of PBHs, one needs a power spectrum with a smaller peak amplitude. This argument implies that the presence of primordial non-Gaussianity will tend to decrease the relevance of the one-loop corrections.

⁴There is some difference between peak theory and threshold statistics in the computation of the abundance, already present at the Gaussian level (see, e.g., Refs. [62,77,78]). The approach based on peak theory usually requires slightly smaller values of $\mathcal{P}_{\text{USR}}/\mathcal{P}_{\text{CMB}}$ in order to get the same abundance of PBHs, thus making our findings, based on threshold statistics, even stronger.

panel of Fig. 3. Reference [79] computed one-loop corrections in the limit of instantaneous SR/USR/SR transitions in scenarios with $\eta_{\text{II}} \leq 3$, finding that the perturbativity bound is relaxed for η_{II} smaller than 3. At a qualitative level, similar results are obtained in the left panel of Fig. 4. In Ref. [79], the perturbativity bound is traduced in an upper limit on the power spectrum at the scale k_{end} . However, as explained above, this procedure underestimates the maximum amplitude of the power spectrum, see again the left panel of Fig. 3.

3. Dynamics at the SR/USR/SR transition

We go beyond the instantaneous transition to check if there are cancellations that affect the order-of-magnitude of the result in Eq. (88). There are indeed compelling reasons to believe that this is the case, as advocated in Refs. [38–40]. The story goes as follows (the original argument was proposed in Ref. [65] in which the role of non-Gaussianity from nonattractor inflation models was considered). From the Hubble parameters in Eq. (2) and the background dynamics that follow from the action in Eq. (4), it is possible to calculate the potential and its derivatives exactly. Up to the third order in field derivatives, we find (see also Ref. [80])

$$V(\phi) = H^2(3 - \epsilon), \quad (91)$$

$$V'(\phi) = \frac{H^2}{\sqrt{2}} \epsilon^{1/2} (6 - 2\epsilon + \epsilon_2), \quad (92)$$

$$V''(\phi) = H^2 \left(6\epsilon - 2\epsilon^2 - \frac{3\epsilon_2}{2} + \frac{5\epsilon\epsilon_2}{2} - \frac{\epsilon_2^2}{4} + \frac{\epsilon_2\epsilon_3}{2} \right), \quad (93)$$

$$V'''(\phi) = \frac{H^2}{2\sqrt{2}\epsilon} \left[-8\epsilon^3 + 6\epsilon^2(4 + 3\epsilon_2) - \epsilon\epsilon_2(18 + 6\epsilon_2 + 7\epsilon_3) + \epsilon_2\epsilon_3(3 + \epsilon_2 + \epsilon_3 + \epsilon_4) \right] \quad (94)$$

$$= \frac{1}{2\sqrt{2}\epsilon} \left\{ H^2 \left[\frac{\ddot{\epsilon}_2}{H^2} + (3 + \epsilon_2) \frac{\dot{\epsilon}_2}{H} \right] + O(\epsilon) \right\}, \quad (95)$$

where in Eq. (95) we expanded in the parameter ϵ and wrote $\epsilon_{3,4}$ in terms of ϵ_2 . Consider the flat gauge in which curvature perturbations are entirely encoded into field fluctuations $\delta\phi$ by means of the relation $\zeta = H\delta\phi/\dot{\phi} = -\delta\phi/\sqrt{2\epsilon}$. In this gauge, the interactions come from Taylor-expanding the quadratic action in field fluctuations and, at the cubic order, one expects

$$\begin{aligned} \mathcal{L}_3 \supset \frac{a^3}{6} V''' \delta\phi^3 &= -\frac{a^3\epsilon}{3} (\sqrt{2\epsilon} V''') \zeta^3 \\ &= -\frac{a^3\epsilon}{6} \left\{ H^2 \left[\frac{\ddot{\epsilon}_2}{H^2} + (3 + \epsilon_2) \frac{\dot{\epsilon}_2}{H} \right] + O(\epsilon) \right\} \zeta^3. \end{aligned} \quad (96)$$

As shown in Ref. [64], the above interaction agrees (modulo a surface term) with Eq. (42) if we integrate by parts

$$\begin{aligned} \int d^4x \frac{\epsilon\dot{\epsilon}_2}{2} a^3 \zeta^2 &\rightarrow - \int d^4x \frac{1}{6} \frac{d}{dt} (\epsilon\dot{\epsilon}_2 a^3) \zeta^3 \\ &= - \int d^4x \frac{a^3\epsilon}{6} H^2 \left[\frac{\ddot{\epsilon}_2}{H^2} + (3 + \epsilon_2) \frac{\dot{\epsilon}_2}{H} \right] \zeta^3, \end{aligned} \quad (97)$$

where in the last step we used the exact identity

$$\frac{d}{dt} (\epsilon\dot{\epsilon}_2 a^3) = a^3 \epsilon H^2 \left[\frac{\ddot{\epsilon}_2}{H^2} + (3 + \epsilon_2) \frac{\dot{\epsilon}_2}{H} \right]. \quad (98)$$

The cubic interaction in Eq. (97) agrees with Eq. (96) up to ϵ -suppressed terms. Rewriting the interaction as in Eq. (96) is quite instructive. From Eq. (98), it seems plausible that drastic variations in time of ϵ_2 could enhance the cubic interaction. However, Eq. (96) shows that these interactions are ultimately controlled by V''' so that in the case with a smooth SR/USR/SR transition in which V''' is expected to be “small,” there must be cancellations at work within the combination in Eq. (98) so that the relevant coupling in Eq. (96) reduces to the term that is SR suppressed. This is the main argument that was put forth in Refs. [38–40].

We shall elaborate further on this point. First of all, let us clarify what “ V''' small” means. We rewrite Eq. (95) as follows [we omit the $O(\epsilon)$ terms and, for clarity’s sake, we write explicitly the reduced Planck mass]

$$\frac{V'''}{H} = \left(\frac{H}{\bar{M}_{\text{Pl}}} \right) \frac{1}{2\sqrt{2}\epsilon} \left[\frac{\ddot{\epsilon}_2}{H^2} + (3 + \epsilon_2) \frac{\dot{\epsilon}_2}{H} \right]. \quad (99)$$

On the left-hand side, the quantity V'''/H has the dimension of a coupling. Consequently, imposing the condition $V'''/H < 1$ corresponds to a weak coupling regime while $V'''/H > 1$ corresponds to a strongly coupled one. Said differently, from the perspective of the right-hand side of Eq. (99), the condition $V'''/H > 1$ corresponds to a situation in which the a-dimensional factor in front of H/\bar{M}_{Pl} becomes so large that it overcomes the natural suppression given by $H/\bar{M}_{\text{Pl}} \ll 1$. In the left panel of Fig. 5, we compute the ratio V'''/H for two benchmark SR/USR/SR dynamics with different values of δN . In the case in which $\delta N \rightarrow 0$ (sharp transition), we observe that V'''/H dangerously grows towards the strongly coupled regime while in the case of a smooth transition it safely takes $O(\ll 1)$ values. As anticipated at the beginning of this section, this argument confirms that in the case of a smooth transition we expect a reduction in the size of the trilinear interaction controlled by the factor in Eq. (98).

With this motivation in mind, we go back to the analysis in Sec. IV A 1 and we perform the following calculation.

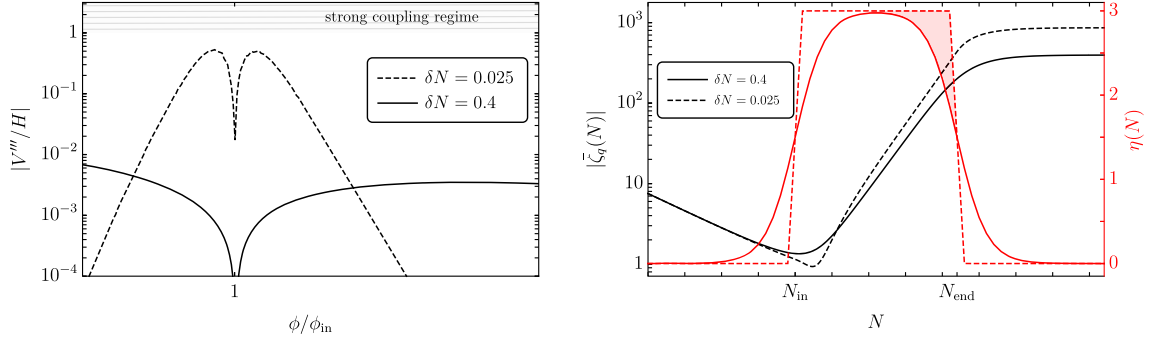


FIG. 5. Left panel: graph of V'''/H as function of the background field value ϕ for two representative dynamics with, respectively, $\delta N = 0.025$ (dashed black) and $\delta N = 0.4$ (solid black). Starting from the dynamics defined as in Sec. II B, we compute the potential by means of the reverse engineering approach described in Ref. [54]. The values V_\star and H_\star of, respectively, the potential and the Hubble rate at CMB scales are chosen in such a way that both dynamics are consistent with CMB observations (namely, $V_\star \simeq 3 \times 10^{-9}$ and $H_\star \simeq 3 \times 10^{-5}$ with the reduced Planck mass set to 1). On the right (left) side of the field value $\phi = \phi_{\text{in}}$, V'''/H is negative (positive). Right panel: left-side y axis: time evolution of the curvature modes $|\bar{\zeta}_q(N)|$ for $\bar{q} = 2$ in the case $\delta N = 0.025$ (dashed black line) and $\delta N = 0.4$ (solid black line). Right-side y axis: profile of η in the case $\delta N = 0.025$ (dashed red line) and $\delta N = 0.4$ (solid red line). The region shaded in red highlights the difference between the sharp and the smooth transition in terms of η : in the case of a sharp transition, the curvature mode has more time to grow under the effect of the negative friction phase implied by the condition $\eta > 3/2$.

We compute numerically the integral in Eq. (79) in order to check the validity of the scaling in Eq. (88) beyond the limit of instantaneous transition. We define the quantity

$$\begin{aligned} \mathcal{J}_{\delta N}(\eta_{\text{II}}, \Delta N_{\text{USR}}) &\equiv \Delta \mathcal{P}_{\text{1-loop}}(k_*) / \mathcal{P}_{\text{tree}}(k_*) \\ &= 32 \int_{N_{\text{in}} - \Delta N}^{N_{\text{end}} + \Delta N} dN_1 \frac{d\eta}{dN}(N_1) \int_{N_{\text{in}} - \Delta N}^{N_1} dN_2 \bar{\epsilon}(N_2) \frac{d\eta}{dN}(N_2) e^{3(N_2 - N_{\text{in}})} \\ &\quad \times \int_1^{e^{\Delta N_{\text{USR}}}} \frac{d\bar{q}}{\bar{q}^4} \text{Im} \left[\bar{\zeta}_q(N_1)^2 \bar{\zeta}_q^*(N_2) \frac{d\bar{\zeta}_q^*}{dN}(N_2) \right], \end{aligned} \quad (100)$$

that we can directly compare, in the case $\eta_{\text{II}} = 3$, with $\eta_{\text{II}}^2 (k_{\text{end}}/k_{\text{in}})^6 [1 + \log(k_{\text{end}}/k_{\text{in}})]$ in Eq. (88) using the fact that $k_{\text{end}}/k_{\text{in}} = e^{\Delta N_{\text{USR}}}$. First, we set δN to a very small number, in order to mimic the limit $\delta N \rightarrow 0$, and evaluate $\mathcal{J}_{\delta N}(3, \Delta N_{\text{USR}})$ as function of ΔN_{USR} . The comparison is

shown in the left panel of Fig. 6. We find an excellent agreement in particular for large ΔN_{USR} . This is expected, since the approximation in Eq. (87) is more accurate for larger $k_{\text{end}}/k_{\text{in}}$. Then, we set $\Delta N_{\text{USR}} = 3$ and compare the value of $\mathcal{J}_{\delta N \rightarrow 0}(3, 3)$ with $\mathcal{J}_{\delta N}(3, 3)$ as function of δN .

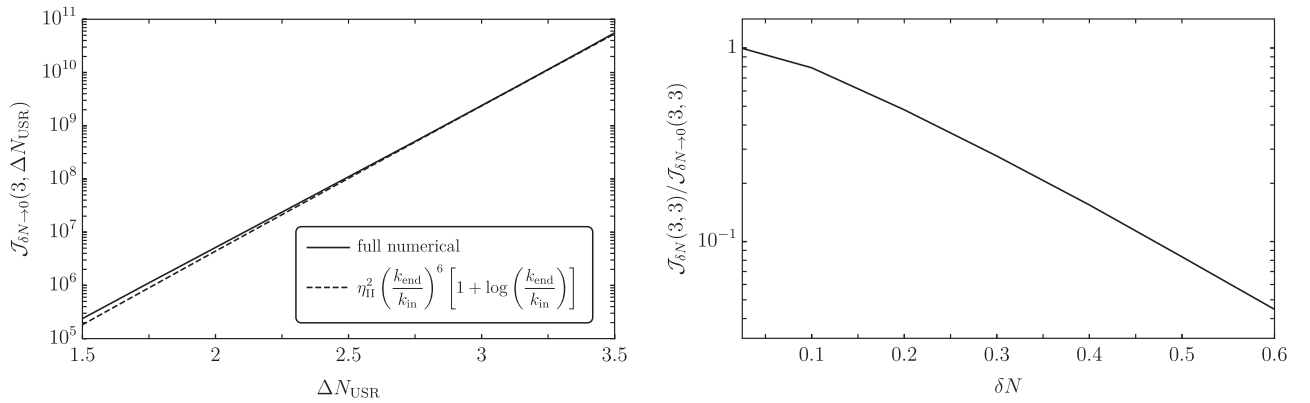


FIG. 6. Left panel: comparison between the value of the full integral in Eq. (100) and the analytical estimate in Eq. (88). To mimic the instantaneous transition we take $\delta N = 0.025$. Right panel: we plot the ratio $\mathcal{J}_{\delta N}(3, \Delta N_{\text{USR}})$ as function of δN . In both figures we take $\eta_{\text{II}} = 3$.

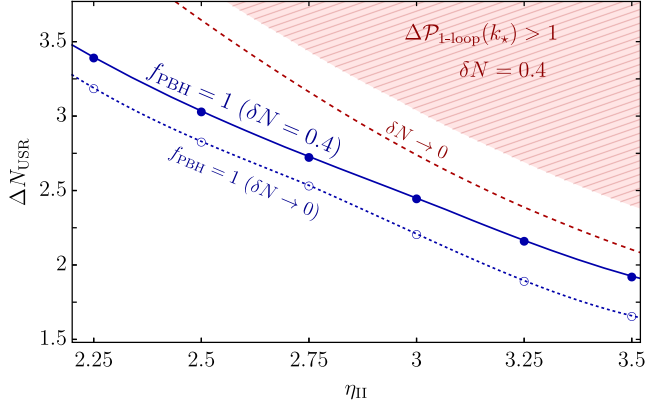


FIG. 7. We consider a generic USR dynamics with varying η_{II} (x axis) and ΔN_{USR} (y axis). We take $\eta_{\text{III}} = 0$ and the smooth limit $\delta N = 0.4$. The region hatched in red corresponds to $\Delta \mathcal{P}_{1\text{-loop}}(k_*) > 0$. Along the line defined by the condition $f_{\text{PBH}} = 1$, we get 100% of DM in the form of asteroid-mass PBHs. The dotted blue line and the red dashed line correspond, respectively, to the conditions $f_{\text{PBH}} = 1$ and $\lim_{\delta N \rightarrow 0} \Delta \mathcal{P}_{1\text{-loop}}(k_*) > 0$ as derived in the limit of instantaneous transition.

We plot the ratio $\mathcal{J}_{\delta N}(3, 3)/\mathcal{J}_{\delta N \rightarrow 0}(3, 3)$ in the right panel of Fig. 6.

Realistic single-field models that feature the presence of a phase of USR dynamics typically have $\delta N = 0.4 \div 0.5$ (cf., e.g., Ref. [12,53]). This means that, according to our result in the right panel of Fig. 6, we expect that in realistic models the size of the loop correction gets reduced by one order of magnitude with respect to what is obtained in the limit of instantaneous SR/USR/SR transition. This confirms the intuition presented in Refs. [38].

It should be noted, however, as evident from our discussion in Sec. II B, that in the case of smooth SR/USR/SR transition the amplitude of the power spectrum gets reduced with respect to the $\delta N \rightarrow 0$ limit (cf. the left panel of Fig. 3). The origin of this effect becomes evident if we consider the right panel of Fig. 5. In this figure, we plot

the time evolution of the curvature mode $|\tilde{\zeta}_q|$ with $\bar{q} = 2$ in the two cases of a sharp and smooth transition (dashed and solid lines, respectively, see caption for details). In the case of a sharp transition, the curvature mode experiences a longer USR phase, and its final amplitude is larger with respect to the case of a smooth transition. As a consequence, therefore, we expect that the smaller size of the loop correction will be, at least partially, compensated by the fact that finite δN also reduces the amplitude of the tree-level power spectrum. In order to quantify this information, we repeat the analysis done in Sec. IV A 2 but now for finite δN . We plot our result in Fig. 7. For definiteness, we consider the benchmark value $\delta N = 0.4$ while we keep η_{II} and ΔN_{USR} generic as in Fig. 4.

Our numerical analysis mirrors the previous intuition. The perturbativity bound (the region hatched in red corresponds to the condition $\Delta \mathcal{P}_{1\text{-loop}}(k_*) > 0$) gets weaker because of the partial cancellation illustrated in the right panel of Fig. 6. However, as previously discussed, the drawback is that taking $\delta N \neq 0$ also reduces the peak amplitude of the power spectrum. Consequently, the condition $f_{\text{PBH}} = 1$ requires, for fixed η_{II} , larger ΔN_{USR} .

As for the limit of instantaneous transition, the condition $f_{\text{PBH}} = 1$ does not violate the perturbativity bound since the two above-mentioned effects nearly compensate each other. However, our analysis reveals an interesting aspect: modeling the SR/USR/SR transition (and, in particular, the final USR/SR one) beyond the instantaneous limit reduces the impact of the loop correction but, at the same time, lowers the peak amplitude of the tree-level power spectrum, which must be compensated by a larger ΔN_{USR} see Fig. 8. As illustrated in Fig. 7, both these effects must be considered together in order to properly quantify the impact of loop corrections and the consequent perturbativity bound.

This is an interesting point. References [38–40] argue that if one goes beyond the limit of instantaneous transition then the loop correction to the CMB power spectrum becomes effectively harmless. Technically speaking, in

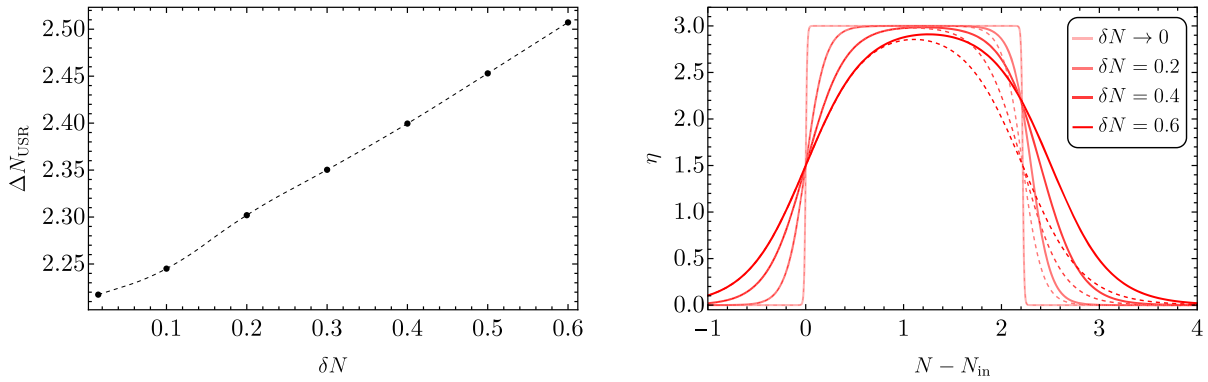


FIG. 8. Left panel: value of ΔN_{USR} required in order to have $f_{\text{PBH}} = 1$ for $\eta_{\text{II}} = 3$. Right panel: different examples of evolution of $\eta(N)$ responsible for the USR, assuming various δN and fixing $\eta_{\text{II}} = 3$. Dashed lines reports the scenario where δN is increased while ΔN_{USR} is kept fixed to the value imposed to have unit PBH abundance in the limit $\delta N \rightarrow 0$. Solid lines report the result when ΔN_{USR} is instead adjusted to keep $f_{\text{PBH}} = 1$ fixed. We see that smoother transitions results in longer USR phases.

our analysis the role of the parameter $-6 < h < 0$ that in [38–40] (see also Ref. [65]) controls the sharpness of the transition is played by our parameter δN (with $h \rightarrow -6$ that corresponds to our $\delta N \rightarrow 0$ and $h \rightarrow 0$ that corresponds to increasing values of δN).

In light of our analysis, a very important remark naturally arises: There is a nontrivial and crucial interplay between the detail of the USR/SR transition and the amplitude of the tree-level power spectrum that must be properly included before drawing any conclusion about the relative size of the loop corrections. On the one hand, it is true that a smooth USR/SR transition reduces the size of the loop correction; on the other one, the same smoothing also reduces the amplitude of the power spectrum so that, in order to keep f_{PBH} fixed, one is forced to either increase the duration of the USR phase or the magnitude of η during the latter. In the end, the two effects tend to compensate each other if one imposes the condition $f_{\text{PBH}} = 1$ (cf. Fig. 7).

B. Loop evaluation at any scales

We evaluate the loop correction at a generic external momentum k , thus alleviating the assumption $k \ll q$. The

dominant modes contributing to the loop integration remain the ones that cross the horizon during the USR phase $q \in [k_{\text{in}}, k_{\text{end}}]$. As done in the previous section, we are interested in comparing the one-loop correction with the tree level power spectrum at the end of inflation, and therefore we perform the late time limit $\tau \rightarrow 0^-$. Following the notation introduced in Eq. (54), we define

$$\begin{aligned} \mathcal{P}(k) &= \lim_{\tau \rightarrow 0^-} \left(\frac{k^3}{2\pi^2} \right) \left[|\zeta_k(\tau)|^2 + \frac{1}{(4\pi)^2} \Delta P(k, \tau) \right] \\ &\equiv \mathcal{P}_{\text{tree}}(k) (1 + \Delta \mathcal{P}_{1\text{-loop}}). \end{aligned} \quad (101)$$

In order to simplify the computation we consider the instantaneous limit $\delta N \rightarrow 0$ of Eq. (77). We perform both time integrations keeping the dominant contribution given by the first Dirac delta in Eq. (31). This implies that we evaluate the integrand function at $\tau_1 = \tau_2 = \tau_{\text{end}}$. Notice also that, since the second integration only gets contributions from half of the Dirac delta domain, we additionally include a factor of $1/2$. Finally, the jump in ϵ_2 leaves a factor $(2\eta_{\text{II}})$ for each time integration. Therefore, we find

$$\begin{aligned} \Delta P(k, \tau) &\equiv -32\eta_{\text{II}}^2 [\epsilon(\tau_{\text{end}}) a^2(\tau_{\text{end}})]^2 \int_{q_{\text{in}}}^{q_{\text{end}}} dq q^2 \int_{-1}^1 d(\cos \theta) \\ &\times \{ \text{Im}[\zeta_k^*(\tau) \zeta_k'(\tau_{\text{end}})] \times [\text{Im}[\zeta_k(\tau) \zeta_k'^*(\tau_{\text{end}}) |\zeta_q(\tau_{\text{end}})|^2 |\zeta_{k-q}(\tau_{\text{end}})|^2] \\ &+ \text{Im}[\zeta_k(\tau) \zeta_k^*(\tau_{\text{end}}) (|\zeta_q(\tau_{\text{end}})|^2 \zeta_{k-q}(\tau_{\text{end}}) \zeta_{k-q}'^*(\tau_{\text{end}}) + |\zeta_{k-q}(\tau_{\text{end}})|^2 \zeta_q(\tau_{\text{end}}) \zeta_q'^*(\tau_{\text{end}}))] \\ &+ \text{Im}[\zeta_k^*(\tau) \zeta_k(\tau_{\text{end}})] \times [\text{Im}[\zeta_k(\tau) \zeta_k'^*(\tau_{\text{end}}) (|\zeta_q(\tau_{\text{end}})|^2 \zeta_{k-q}^*(\tau_{\text{end}}) \zeta_{k-q}'(\tau_{\text{end}}) + |\zeta_{k-q}(\tau_{\text{end}})|^2 \zeta_q^*(\tau_{\text{end}}) \zeta_q'(\tau_{\text{end}}))] \\ &+ \text{Im}[\zeta_k(\tau) \zeta_k^*(\tau_{\text{end}}) (|\zeta_{k-q}'(\tau_{\text{end}})|^2 |\zeta_q(\tau_{\text{end}})|^2 + \zeta_{k-q}'(\tau_{\text{end}}) \zeta_{k-q}^*(\tau_{\text{end}}) \zeta_q(\tau_{\text{end}}) \zeta_q'^*(\tau_{\text{end}}))] \\ &+ \text{Im}[\zeta_k(\tau) \zeta_k^*(\tau_{\text{end}}) (|\zeta_{k-q}'(\tau_{\text{end}})|^2 |\zeta_q(\tau_{\text{end}})|^2 + \zeta_{k-q}'^*(\tau_{\text{end}}) \zeta_{k-q}(\tau_{\text{end}}) \zeta_q^*(\tau_{\text{end}}) \zeta_q'(\tau_{\text{end}}))] \}. \end{aligned} \quad (102)$$

We have collected the pieces such that each line corresponds to the i th term in the sum of Eq. (77) and $k - q \equiv \sqrt{k^2 + q^2 - 2kq \cos(\theta)}$ as in the previous section.

In the left panel of Fig. 9, we show the resulting one-loop correction as a function of the wave number k for a representative set of parameters leading to $f_{\text{BH}} \approx 1$: $\eta_{\text{II}} = 3$ and $\Delta N_{\text{USR}} = 2.2$. We find values of $\Delta \mathcal{P}_{1\text{-loop}}$ of the order of few percent, barring small oscillatory features. A notable exception is the scale where the tree level power spectrum presents a dip, see Fig. 3, $k_{\text{dip}}/k_{\text{in}} \approx \sqrt{5/4} e^{-3\Delta N_{\text{USR}}/2}$ [52]. At that scale the one-loop correction dominates, resulting in a spike in $\Delta \mathcal{P}_{1\text{-loop}}$. As a consequence, the dip is only realized if the one-loop correction is neglected, see the right panel of Fig. 9. We also observe that in the limit of small $k \ll k_{\text{in}}$ the result quickly converges towards the one discussed in the previous section, as expected. Finally, it is also interesting to notice that the correction $\Delta \mathcal{P}_{1\text{-loop}}$ stays almost the same at any scale, except around k_{dip} .

For this reason, we expect that a generalization of this calculation to the case for $\delta N \neq 0$ will lead to results similar to ones presented in the previous section for $k \ll q$.

At first sight, our result that loop corrections impact the tree-level power spectrum at the percent level seems at odds with the findings of Ref. [58] in which it was found that the one-loop power spectrum could dominate over the tree-level one, thus indicating the breakdown of the perturbation theory. Upon a closer look, however, there is no contradiction. Reference [58] considers a particular instance of background dynamics in which curvature perturbations are resonantly amplified due to a specific pattern of oscillatory features in the inflaton potential. In such a model, we checked that the condition $V'''/H \ll 1$ [cf. Eq. (99) and the related discussion] is not verified and, therefore, it is not unexpected to find an amplification of loop effects.

It is instructive to consider also a different limit. Since we are assuming that the USR is followed by a second period of slow roll, characterized by a negligible η_{III} and a small ϵ ,

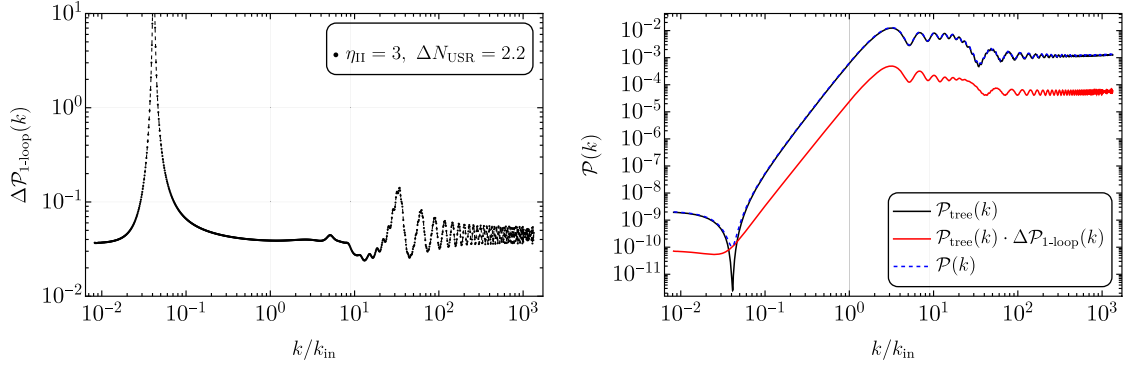


FIG. 9. In both panels, we consider a USR dynamics with $\eta_{\text{II}} = 3$, $\Delta N_{\text{USR}} = 2.2$, $\eta_{\text{III}} = 0$ and the instantaneous limit $\delta N = 0$. These values corresponds to a scenario producing $f_{\text{PBH}} \simeq 1$. The vertical gridlines corresponds to $k = k_{\text{in}}$ and k_{end} in both panels. Left panel: correction to the tree level power spectrum as a function of k in the limit of $\tau \rightarrow 0^-$. Right panel: tree level power spectrum (black) compared to the one-loop correction (red line) and their sum (blue dashed line).

modes in the range $q \in [k_{\text{in}}, k_{\text{end}}]$ freeze around τ_{end} . Therefore, the loop correction at τ_{end} is very close to its limit at $\tau \rightarrow 0^-$, as we verified through a numerical calculation. For this reason, we set $\tau \rightarrow \tau_{\text{end}}$ in Eq. (102) and drop the factors proportional to $\text{Im}[\zeta_k^*(\tau_{\text{end}})\zeta_k(\tau_{\text{end}})]$

which vanish identically. Next, we switch to the barred fields and momenta notation introduced in Sec. IV A and simplify the expression using the Wroksian identity (82). Finally, we arrive at the expression

One-loop correction at generic scales in the instantaneous SR/USR/SR transition

$$\lim_{\delta N \rightarrow 0} \Delta \mathcal{P}_{1\text{-loop}}(k, \tau_{\text{end}}) \approx 4\eta_{\text{II}}^2 \left(\frac{H^2}{8\pi^2 \epsilon_{\text{ref}}} \right) \frac{1}{|\bar{\zeta}_k(N_{\text{end}})|^2} \int_1^{e^{\Delta N_{\text{USR}}}} \frac{d\bar{q}}{\bar{q}} \int_{-1}^{+1} d(\cos \theta) \times \left\{ \frac{\bar{k}^3}{(\bar{k} - \bar{q})^3} |\bar{\zeta}_q(N_{\text{end}})|^2 |\bar{\zeta}_{k-q}(N_{\text{end}})|^2 + |\bar{\zeta}_k(N_{\text{end}})|^2 \left[|\bar{\zeta}_q(N_{\text{end}})|^2 + \frac{\bar{q}^3}{(\bar{k} - \bar{q})^3} |\bar{\zeta}_{k-q}(N_{\text{end}})|^2 \right] \right\}. \quad (103)$$

We stress that this result is exact in the limit of sharp transition $\delta N \rightarrow 0$ and only neglects the contribution from the integration of the step function in N_{in} , which is numerically subleading.

A number of important comments are in order.

- (i) In the case in which k is a long CMB mode ($k \ll q$), the first term in the curly brackets is suppressed by the factor $(k/q)^3$. This is nothing but the number of independent Hubble patches of size q^{-1} in a box of radius k^{-1} . Intuitively, therefore, this contribution represents the situation in which random small-scale fluctuations lead by chance to a large-scale fluctuation, and the suppression factor $(k/q)^3$ simply indicates that it is very unlucky for short-mode to be coherent over long scales. The meaning of this term is very clear, and the above argument is so

compelling that it forces the intuition to believe that there is no way in which CMB modes can be affected by small-scale ones.

It is worth emphasizing that the computation of the one-loop correction to the correlation of long-wavelength modes k due to short modes q running in the loop can be thought of as solving the nonlinear evolution equation for the long mode, cf. Refs. [36,46]. In the language of this *source method*, the first term in the curly brackets of Eq. (103) corresponds to the so-called cut-in-the-middle diagrams, cf. Ref. [81]. It also corresponds to the Poisson-suppressed term identified in Ref. [36] while, in the language of Ref. [37], it corresponds to the correlation of two inhomogeneous solutions. More in detail, the evolution of the long mode in the presence of interactions reads

$$\hat{\zeta}(\vec{k}, N_f) = \underbrace{\hat{\zeta}(\vec{k}, N_{\text{in}}) + a^3(N_{\text{in}})\epsilon(N_{\text{in}}) \frac{d\hat{\zeta}}{dN}(\vec{k}, N_{\text{in}})}_{\text{homogeneous solution (free evolution)}} \int_{N_{\text{in}}}^{N_f} dN \frac{1}{a^3(N)\epsilon(N)} \quad (104)$$

$$\underbrace{-\frac{\eta_{\text{II}}}{2} \int \frac{d^3 \vec{q}}{(2\pi)^3} \hat{\zeta}(\vec{q}, N_{\text{end}}) \hat{\zeta}(-\vec{q}, N_{\text{end}}) + \frac{\eta_{\text{II}}}{3} \int \frac{d^3 \vec{q}}{(2\pi)^3} \frac{d\hat{\zeta}}{dN}(\vec{q}, N_{\text{end}}) \hat{\zeta}(-\vec{q}, N_{\text{end}})}_{\text{inhomogeneous solution (interactions)}}, \quad (105)$$

where N_f represents some final e -fold time after the end of the USR phase. Consider the terms in the first line, Eq. (104). This is the standard result in the absence of interactions (the homogeneous solution in Ref. [37]). Equation (104) tells us that the long mode stays constant unless the duration of the USR phase is so long to overcome the smallness of the time derivative of the long mode, which decayed exponentially fast during the phase preceding the USR. Equation (104), therefore, gives the standard tree-level power spectrum if one computes the correlator $\langle \hat{\zeta}(\vec{k}, N_f) \hat{\zeta}(-\vec{k}, N_f) \rangle$. The two terms in Eq. (105) corresponds to the inhomogeneous solution in Ref. [37], and encode the effect of the interactions in the evolution of the long mode. The first term in the curly brackets of our Eq. (103) corresponds to the correlator of two inhomogeneous solutions. The equivalence between the source method and the “*in-in*” formalism has been discussed explicitly in Ref. [37].

- (ii) Consider now the second term in the curly brackets of Eq. (103). Notice that this term always factorizes $|\zeta_k|^2$ that cancels the denominator in front of the integral, which is present because of our definition of $\Delta\mathcal{P}_{1\text{-loop}}$, cf. Eq. (101). In the case in which k is a long CMB mode ($k \ll q$), this term does not pay any $(k/q)^3$ suppression. In the language of the source method, it corresponds to the so-called cut-in-the-side diagrams, cf. Ref. [46]. These diagrams represent the evolution of the long mode due to the effect that the long mode itself has on the expectation value of quadratic operators made of short modes [46] (cf. Sec. V). In Ref. [37], the second term in the curly brackets of Eq. (103) follows from the correlation between inhomogeneous and homogeneous solutions.

V. DISCUSSION AND OUTLOOK

In this work, we discussed the implications of perturbativity in the context of single-field inflationary models that feature the presence of a transient phase of USR. More in detail, we defined the perturbativity condition

$$\mathcal{P}(k) \equiv \mathcal{P}_{\text{tree}}(k)[1 + \Delta\mathcal{P}_{1\text{-loop}}(k)] \Rightarrow \Delta\mathcal{P}_{1\text{-loop}}(k) \stackrel{!}{<} 1, \quad (106)$$

in which the one-loop correction is integrated over the short modes that are enhanced by the USR dynamics. We explored the consequences of Eq. (106) at any scale k

even though the main motivation for our analysis was the recent claim of Ref. [35] according to which the relative size of the loop correction at scales relevant for CMB observations [that is, $k = O(k_*)$ with $k_* = 0.05 \text{ Mpc}^{-1}$] threatens the validity of perturbativity at the point of ruling out the idea of PBH formation via USR dynamics in single-field inflation.

In this section, we summarize the main results and limitations of our analysis and we will discuss future prospects:

- (1) In the limit of instantaneous SR/USR/SR transition, we confirm the computation of the 1-loop corrections of Ref. [35]. However, we provide a more detailed and precise discussion of the theoretical bound that can be obtained by imposing the perturbativity condition in Eq. (106) on the power spectrum of curvature perturbations at CMB scales.

As far as this part of the analysis is concerned, the key difference with respect to Ref. [35] is that we compare the size of the loop correction with an accurate computation of the PBH abundance rather than with the order-of-magnitude estimate of the enhancement of the power spectrum, based on the SR formula, used in Ref. [35]. Our approach, therefore, includes the following effects. (i) First of all, we generalize the USR dynamics for generic values $\eta_{\text{II}} \neq 3$ (cf. Sec. II B for our parametrization of the background dynamics); (ii) the enhancement of the power spectrum at scales relevant for PBH formation is accurately computed by numerically solving the M-S equation rather than using the SR scaling; (iii) by computing the PBH abundance f_{PBH} , we automatically account for the fact that the correct variable that describes PBH formation in the standard scenario of gravitational collapse is the smoothed density contrast rather than the curvature perturbation field, and we include in our computation the full non-linear relation between the two.

As for this part of the analysis, our findings are summarized in Fig. 4. We find that loop corrections remain of the order of few percent and therefore it is not possible to make the bold claim that PBH formation from single-field inflation is ruled out—not even in the limit of instantaneous SR/USR/SR transition.

- (2) We extend the analysis of Ref. [35] by considering a more realistic USR dynamics. In particular, we implement a smooth description of the SR/USR/SR transition. Recently, Refs. [38–40] claimed that

the presence of a smooth transition in the final USR/SR transition makes the loop correction effectively harmless. Our analysis shows that this conclusion could be invalidated by the fact that there is an interplay between the size of the loop correction and the amplitude of the tree-level power spectrum that is needed to generate a sizable abundance of PBHs. On the one hand, it is true that a smooth USR/SR transition reduces the size of the loop correction; on the other one, the same smoothing also reduces the amplitude of the tree-level power spectrum so that, in order to keep f_{PBH} fixed, one is forced to either increase the duration of the USR phase or the magnitude of η during the latter. In the end, the two effects tend to compensate each other. As for this part of the analysis, our findings are summarized in Fig. 7.

- (3) We consider the one-loop correction of short modes to the tree-level power spectrum at any scale. We find that perturbativity is always satisfied in models that account for the condition $f_{\text{PBH}} = 1$.

More quantitatively, we find that the relative size of the loop correction with respect to the tree-level value of the power spectrum does not exceed the level of a few percent. As for this part of the analysis, our findings are summarized in Fig. 9. We point out one notable exception of phenomenological relevance. A generic feature of the USR dynamics is that it produces a characteristic dip in the tree-level power spectrum, as the one observed in the left panel of Fig. 3. The phenomenological consequences of such a putative dip range from CMB μ -space distortions [82] to 21-cm signals [83]. Our analysis shows that the existence of the dip is nothing but an artifact of the tree-level computation, and it is significantly reduced after including loop corrections. This is because, due to the smallness of the tree-level power spectrum around the characteristic wave numbers of the dip, the nonvanishing loop correction gives the dominant contribution. This is illustrated in the right panel of Fig. 9.

At the conceptual level, it remains true that, in the presence of USR dynamics, loop corrections of short modes may sizably affect the power spectrum at CMB scales. This result echoes an issue of naturalness—an infrared quantity (the amplitude of the curvature power spectrum at CMB scales) appears to be sensitive, via loop effects, to physics that takes place at much shorter scales (those related to PBH formation)—and clashes with the intuition that physics at such vastly different scales should decouple.

The coupling between short and long modes gives a physical effect for the following reason. As discussed in Sec. IV B, the relevant loop correction to the power spectrum at CMB scales comes from the correlation

between homogeneous and inhomogeneous solutions. This is most easily seen within the source method in which one considers the correlation between a freely evolving long mode and a second long mode which evolves in the presence of interactions, cf. Eq. (105). Borrowing from Ref. [81] (see also Ref. [36]), we write the formal solution of the nonlinear evolution equations for a long wavelength mode ζ_L as $\zeta_L = \hat{O}^{-1}[S[\zeta_S, \zeta_S, \zeta_L]]$, where S represents a generic sum of operators that are quadratic in the short wavelength mode ζ_S and that can also depend on ζ_L if one considers the short modes in the background perturbed by the long mode. More concretely, in our case such a solution is the one given by Eq. (105). The one-loop power spectrum is given by

$$\langle \zeta_L \zeta_L \rangle \sim \langle \hat{O}^{-1}[S[\zeta_S, \zeta_S, \zeta_L = 0]] \hat{O}^{-1}[S[\zeta_S, \zeta_S, \zeta_L = 0]] \rangle + \langle \hat{O}^{-1}[S[\zeta_S, \zeta_S, \zeta_L]] \zeta_L \rangle. \quad (107)$$

The first term represents the effect of the short-scale modes in their unperturbed state (that is, with $\zeta_L = 0$) directly on the power spectrum of the long wavelength mode. This is our first term in Eq. (103). As discussed in Sec. IV B, this term does not alter the long-wavelength correlation since it is very improbable that random short-scale fluctuations coherently add up to induce a long-wavelength correlation. The second term in Eq. (107), on the contrary, correlates a freely evolving long mode ζ_L with the effect that the long mode itself has on the expectation value of quadratic operators made of short modes. Let us explain this point, which is crucial. Consider the schematic in Fig. 10. The key point is the following. In the comoving gauge, the short modes evolve in the background that is perturbed by the long mode. In the limit in which the long mode ζ_L has a wavelength much longer than the horizon, it simply acts as a rescaling of the coordinates since it enters as a local change of the scale factor. This is schematically illustrated in Fig. 10. This figure shows intuitively that the short scales are modulated by the presence of the long mode. The presence of the long mode acts as a rescaling of the coordinates and we can absorb it by rescaling the short-scale momenta $q \rightarrow \tilde{q} = e^{\zeta_L} q$ [36]. If the power spectrum of the short modes is scale invariant, then this rescaling does nothing. However, if the power spectrum of the short modes breaks scale invariance, we schematically have in the loop integral over the short modes, expanding at the first order

$$\begin{aligned} \int \frac{dq}{q} \mathcal{P}(q) &\stackrel{q \rightarrow \tilde{q} = e^{\zeta_L} q}{\Rightarrow} \int \frac{d\tilde{q}}{\tilde{q}} \mathcal{P}(\tilde{q}) = \int \frac{dq}{q} \mathcal{P}(e^{\zeta_L} q) \\ &= \int \frac{dq}{q} \left[\mathcal{P}(q) + \zeta_L \frac{d\mathcal{P}}{dq} q \right] \\ &= \int \frac{dq}{q} \left[\mathcal{P}(q) + \zeta_L \mathcal{P}(q) \frac{d \log \mathcal{P}}{d \log q} \right], \quad (108) \end{aligned}$$

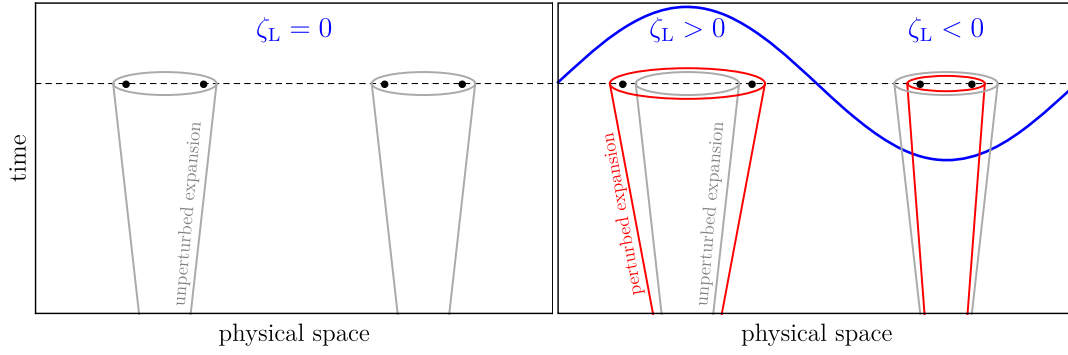


FIG. 10. Left panel: expansion in time of the unperturbed universe (time passes by along the y axis); the Universe expands by the same amount at every point. Right panel: expansion in time of the perturbed universe. The long mode (ζ_L , blue) acts as a local rescaling of the scale factor, and short scales are modulated accordingly. More specifically, if we consider the black dots we see that they experience a different amount of expansion depending on the value of ζ_L .

so that the presence of the long mode affects the correlation of short modes when their power spectrum is not scale invariant. The second term in the above equation describes precisely the effect put forth before: the presence of the long mode alters the expectation value of quadratic operators made of short modes, in this case the short-mode two-point function. This result seems to violate the separate universe conjecture as also shown in Refs. [84,85]. This conjecture states that, in single field inflation models, the curvature perturbation in the superhorizon limit only acts as a rescaling of the spatial coordinates (see, e.g., Refs. [86,87]) and therefore a local observer in a Hubble horizon patch cannot measure the superhorizon-limit curvature perturbations because it can be absorbed into a rescaling of the spatial coordinates. Indeed the separate universe conjecture is limited to the case of single-clock inflation. The term single-clock inflation usually refers to the most general form for the inflationary action (typically constructed through the effective field theory approach) that is consistent with unbroken spatial diffeomorphisms and the presence of a preferred temporal coordinate that

represents the “clock” during inflation (time diffeomorphisms are spontaneously broken). Single-field slow-roll inflation represents the prototypical example of single-clock inflation. The single-clock background is an attractor, and long-wavelength perturbations appear in short-wavelength modes as a constant renormalization of the scale factor that does not affect the local physics.

However USR violates the assumption of an inflationary attractor solution which underlies single-clock inflation. In USR, the field velocity is no longer uniquely determined by the field position and the background is no longer an attractor. To be concrete, we consider in Fig. 11 the phase-space analysis of the SR/USR/SR dynamics presented in Sec. II B, see also Ref. [67] for a similar discussion. First, from the time evolution of ϵ and η we reconstruct the inflationary potential $V(\phi)$ by means of the reverse engineering approach described in Ref. [54]. We then solve the inflaton equation of motion $\ddot{\phi} + 3H\dot{\phi} + V'(\phi) = 0$ and plot the corresponding phase space trajectory (for different initial conditions) in the plane (ϕ, Π) with $\Pi \equiv d\phi/dN$. The dynamics evolves from right to left in Fig. 11. In the left

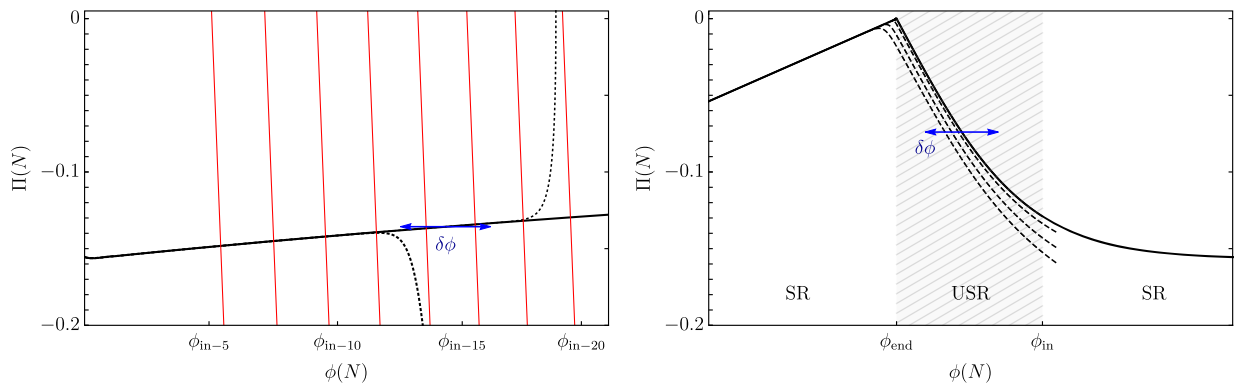


FIG. 11. Left panel: dynamics evolution (from right to the left) of the initial SR phase. The black dotted lines represent two benchmark solutions with large initial velocities, rapidly attracted by the SR trajectory (solid black line). Right panel: dynamics evolution in presence of a USR phase. The background trajectory ceases to be an attractor. Here, the perturbation $\delta\phi$ in the field direction has the effect of altering the background trajectory in phase space, as indicated by the dashed black lines.

panel of Fig. 11 we plot the initial SR phase. The attractor nature of SR is evident. The black dotted lines correspond to two benchmark solutions with large initial velocities. As shown in the plot, they are attracted exponentially fast by the SR trajectory (black solid line). Consequently, if we consider some perturbation $\delta\phi$ in the field direction (which can be thought as a long-wavelength curvature perturbation in the flat gauge) we remain anchored to the background trajectory since small deviations in momentum are quickly reabsorbed. As a result, the perturbation $\delta\phi$ can be simply traded for a shift in the number of e -folds (red lines in the right panel of Fig. 11) that allows one to move on the background trajectory. A shift in the number of e -folds is nothing but a constant renormalization of the scale factor. The situation is different when we enter in the USR phase, right panel in Fig. 11. In this case, the background trajectory is no longer an attractor and the perturbation $\delta\phi$ in the field direction has the effect of changing the background trajectory in phase-space (dashed black lines).

Back to Eq. (107), one expects the one-loop correction [36]

$$\Delta\mathcal{P}_{1\text{-loop}}(k) \sim \mathcal{P}(k) \int \frac{dq}{q} \mathcal{P}(q) \frac{d \log \mathcal{P}}{d \log q}. \quad (109)$$

The above discussion shows that the one-loop corrections on long modes do not decouple when the power spectrum of the short modes is not scale invariant. This explains why our correction vanishes in the limit $\eta_{\text{III}} = 0$ in which indeed

the power spectrum does become scale invariant. The breaking of scale invariance is the hallmark of the USR dynamics and, more importantly, a necessary feature in all models of single-field inflation that generate an order-one abundance of PBHs (cf. the intuitive schematic in Fig. 12).

The last, and most important, remark that we would like to stress is the following. The analysis of Ref. [35] triggered an intense debate about ruling out or not the mechanism of PBH formation via USR in single-field inflation (Refs. [37–44]). Following these analysis, we have estimated the one-loop correction to the curvature power spectrum including the contribution of loop momenta between q_{in} and q_{end} , i.e., the window of momenta where the power spectrum peaks. Within this procedure, we find corrections to the tree-level power spectrum at the percent level in the region of parameter space where $f_{\text{PBH}} \approx 1$. Therefore, at first glance, a sizeable abundance of PBHs in USR single-field inflation is not in conflict with perturbativity constraints. On the other hand, the aforementioned corrections are sizeable, and the contribution of short wavelengths to the power spectrum at large scales does not decouple. This suggests that theoretical constraints dictated by the requirement of perturbativity might be important. As a concrete example, we have shown that loop corrections affect the dip in the tree-level power spectrum. Therefore, a more comprehensive analysis is needed.

We identify the following relevant directions. (i) More realistic modeling of the USR dynamics. As discussed in Sec. II B, in realistic single-field inflationary models we

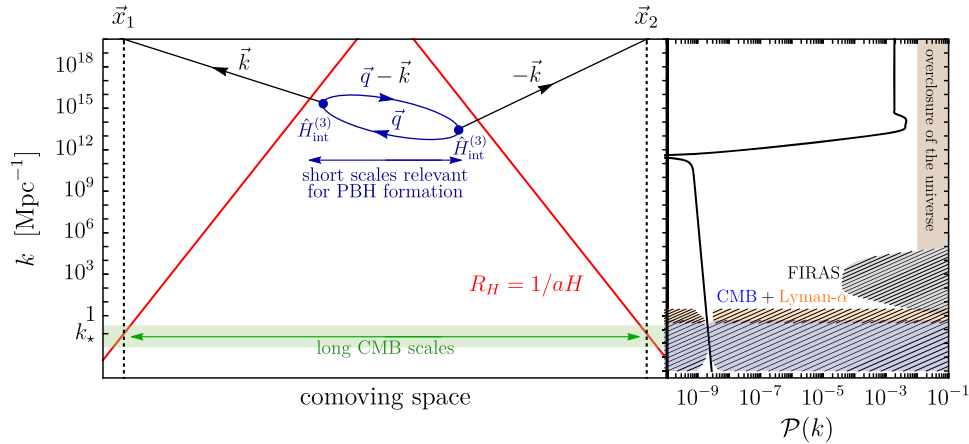


FIG. 12. Illustrative schematic of the correction induced on the two-point correlator of long modes by a loop of short modes. On the right side, we plot the prototypical tree-level power spectrum of curvature perturbations as a function of the comoving wave number k in the presence of SR/USR/SR dynamics (with $\eta_{\text{III}} = 0$ in the language of the parametrization given in Sec. II B). The power spectrum features a strong violation of scale invariance at small scales which is needed in order to produce a sizable abundance of PBHs. For illustration, we plot the region excluded by CMB anisotropy measurements, Ref. [88], the FIRAS bound on CMB spectral distortions, Refs. [89,90] and the bound obtained from Lyman- α forest data [91]. If $\mathcal{P}(k) \gtrsim 10^{-2}$, then the abundance of PBHs overcloses the Universe. The plot is rotated in such a way as to share the same y axis with the left part of the figure. On the left side, we schematically plot the evolution of the comoving Hubble horizon $R_H = 1/aH$ during inflation. Observable CMB modes (horizontal green band) cross the Hubble horizon earlier (bottom-end of the figure) and, at the tree level, their correlation remains frozen from this time on. At a much later time, the dynamics experience a phase of USR. Modes that cross the horizon during the USR phase have their tree-level power spectrum greatly enhanced and the latter strongly violates scale invariance. Loop of such short modes may induce a sizable correction to the tree-level correlation of long modes, cf. Eq. (109).

expect $\eta_{\text{III}} < 0$ and sizable; this is because at the end of the USR we are left with $\epsilon \ll 1$ but we need $\epsilon = O(1)$ to end inflation. Since $\epsilon \sim e^{-2\eta N}$, we need η large and negative after USR. Consequently, after USR we do not expect a scale-invariant power spectrum and Eq. (109) applies. (ii) Understanding the role of quartic interactions, tadpoles and interactions with spatial derivatives. So far, most of the attention has been focused on the role of the cubic interaction Hamiltonian in Eq. (46). However, as schematically shown in Eq. (26), quartic interactions and non-1PI diagrams involving tadpoles are also present. In particular, the schematic in Eq. (26) shows that tadpole diagrams may be relevant because, by attaching them to propagators, they modify the two-point correlator. The correct way to deal with tadpoles is by changing the background solution (cf. Ref. [46]; see also Ref. [58]). Since it is well-known that background solutions in USR models for PBH formation suffer a high-level of parametric tuning (cf. Ref. [92]), the role of tadpole corrections may have some relevance. Furthermore, all interactions with spatial derivatives have been so far discarded. However, the short modes running in the loop cross the horizon precisely during the USR phase and, therefore, their spatial derivatives do not pay any super-horizon suppression. (iii) Renormalization. An essential future step is to implement a thorough renormalization procedure in the context of USR dynamics, a topic that has not yet been addressed in the existing literature.

We will tackle all the above points in a forthcoming work.

ACKNOWLEDGMENTS

We thank C. Byrnes, S. Balaji, G. Fabbian, J. Fumagalli, G. Tasinato and H. Veermäe for discussions and A. Riotto for interesting discussions and comments on the draft. The research of A. U. was supported in part by the MIUR under

Contract No. 2017FMJFMW (“New Avenues in Strong Dynamics,” PRIN 2017). G. F. acknowledges financial support provided under the European Union’s H2020 ERC, Starting Grant Agreement No. DarkGRA-757480 and under the MIUR PRIN programme, and support from the Amaldi Research Center funded by the MIUR program “Dipartimento di Eccellenza” (CUP: B8I18001170001). This work was supported by the EU Horizon 2020 Research and Innovation Programme under the Marie Skłodowska-Curie Grant Agreement No. 101007855 and additional financial support provided by “Progetti per Avvio alla Ricerca—Tipo 2,” protocol number AR2221816C515921. A.J.I. acknowledges additional financial support provided under the “Progetti per Avvio alla Ricerca Tipo 1,” protocol number AR12218167D66D36. M. T. acknowledges the research grant “The Dark Universe: A Synergic Multimessenger Approach No. 2017X7X85” funded by MIUR, and the project “Theoretical Astroparticle Physics (TAsP)” funded by Istituto Nazionale di Fisica Nucleare (INFN).

APPENDIX: DYNAMICS OF CURVATURE MODES, SOME ESSENTIAL RESULTS

The main purpose of this appendix is to understand, both numerically and analytically, the behavior of the time derivative $d\zeta_k/dN$.

We rewrite the M-S equation in the form

$$\frac{d^2\zeta_k}{dN^2} + (3 + \epsilon - 2\eta) \frac{d\zeta_k}{dN} + \frac{k^2}{(aH)^2} \zeta_k = 0. \quad (\text{A1})$$

Assuming $\epsilon \approx 0$, constant η and constant H , this equation admits the solution

$$\zeta_k(N) \propto e^{-(\frac{3}{2}-\eta)N} \left[c_1 J_{\frac{3}{2}-\eta}(\bar{k}e^{N_{\text{in}}-N}) \Gamma\left(\frac{5}{2}-\eta\right) + c_2 J_{-\frac{3}{2}+\eta}(\bar{k}e^{N_{\text{in}}-N}) \Gamma\left(-\frac{1}{2}+\eta\right) \right], \quad (\text{A2})$$

where $J_\alpha(x)$ are Bessel functions of the first kind and $\Gamma(x)$ is the Euler gamma function. Consequently, we find

$$\frac{d\zeta_k}{dN}(N) \propto e^{-(\frac{3}{2}-\eta)N} \left[-c_1 J_{\frac{1}{2}-\eta}(\bar{k}e^{N_{\text{in}}-N}) \Gamma\left(\frac{5}{2}-\eta\right) + c_2 J_{-\frac{1}{2}+\eta}(\bar{k}e^{N_{\text{in}}-N}) \Gamma\left(-\frac{1}{2}+\eta\right) \right]. \quad (\text{A3})$$

This approximation is applicable for $N < N_{\text{in}}$ with $\eta = 0$, for $N_{\text{in}} < N < N_{\text{end}}$ with $\eta = \eta_{\text{II}}$ and for $N > N_{\text{end}}$ with $\eta = \eta_{\text{III}}$. We have the following asymptotic behaviors

$$J_\alpha(x) \sim \begin{cases} 1/\sqrt{x} & \text{for } x \gg 1 \\ x^\alpha & \text{for } x \ll 1 \end{cases} \quad \text{where } x \equiv \bar{k}e^{N_{\text{in}}-N} = e^{N_k-N}. \quad (\text{A4})$$

Consequently, we highlight the following scalings.

(i) On subhorizon scales, we find

$$\text{sub-horizon scales,} \quad N \ll N_k \zeta_k(N) \sim e^{-(1-\eta)N} \quad \text{and} \quad \frac{d\zeta_k}{dN}(N) \sim e^{-(2-\eta)N}. \quad (\text{A5})$$

The above scaling implies, for instance, that before the USR phase (that is, for $N < N_{\text{in}}$ with $\eta = 0$) subhorizon modes decay according to $\zeta_k \sim e^{-N}$ and $d\zeta_k/dN \sim e^{-2N}$.

(ii) On superhorizon scales, we find

$$\text{superhorizon scales,} \quad N \gg N_k \zeta_k(N) \sim c_1 e^{-(3-2\eta)N} + c_2 \quad \text{and} \quad \frac{d\zeta_k}{dN}(N) \sim -c_1 e^{-(3-2\eta)N} + c_2 e^{-2N}. \quad (\text{A6})$$

Consider a mode that is superhorizon after the end of the USR phase (that is, for $N > N_{\text{end}}$ with $\eta = \eta_{\text{III}} < 0$). Equation (A6) tells us that $d\zeta_k/dN$ is given by the superposition of two functions: the first one decays faster, as $e^{-(3-2\eta_{\text{III}})N}$, while the second one decays slower, as e^{-2N} . On the contrary, ζ_k quickly settles to a constant value.

(iii) Consider the evolution during the USR phase. We have $\eta = \eta_{\text{II}} > 3/2$ and $N_{\text{in}} < N < N_{\text{end}}$. We have two possibilities that are relevant to our analysis.

- (1) If the mode is way outside the horizon at the beginning of the USR phase, it stays constant even though its derivative exponentially grows because of the term $\sim e^{-(3-2\eta_{\text{II}})N}$.
- (2) Consider a mode that crosses the Hubble horizon during the USR phase. The curvature perturbation (and its derivative) grows because of the factor $e^{-(3/2-\eta_{\text{II}})N}$. However, it is not immediate to find the exact scaling in time because in this case none of the approximations in Eq. (A4) can be applied.

All the above features, even though obtained in the context of the over-simplified framework given by Eqs. (A2) and (A3), are valid in general. In Fig. 13, we plot $|\zeta_k|$ and $|d\zeta_k/dN|$ using the dynamics presented in Sec. II B. We checked that all the relevant scaling properties discussed above are indeed verified. It is possible to derive some useful analytical approximations.

First of all, we consider the Wronskian condition

$$i[u'_k(\tau)u_k^*(\tau) - u'_k(\tau)u_k(\tau)] = 1, \quad (\text{A7})$$

which we rewrite as

$$i(aH) \left[\frac{du_k}{dN}(N)u_k^*(N) - \frac{du_k^*}{dN}(N)u_k(N) \right] = 1. \quad (\text{A8})$$

As far as du_k/dN is concerned, we find

$$\frac{du_k}{dN} = a\sqrt{2\epsilon}(1 + \epsilon - \eta)\zeta_k + a\sqrt{2\epsilon}\frac{d\zeta_k}{dN}, \quad (\text{A9})$$

so that the Wronskian condition reads

$$\text{Im} \left[\zeta_k(N) \frac{d\zeta_k^*}{dN}(N) \right] = \frac{H^2}{4\epsilon_{\text{ref}}\bar{\epsilon}(N)(aH)^3}. \quad (\text{A10})$$

If we introduce the field $\bar{\zeta}_k$ as in Eq. (81), we find

$$\begin{aligned} W(N) &\equiv \text{Im} \left[\bar{\zeta}_k(N) \frac{d\bar{\zeta}_k^*}{dN}(N) \right] = -\text{Im} \left[\bar{\zeta}_k^*(N) \frac{d\bar{\zeta}_k}{dN}(N) \right] \\ &= \frac{\bar{k}^3}{4\bar{\epsilon}(N)} e^{3(N_{\text{in}}-N)}, \end{aligned} \quad (\text{A11})$$

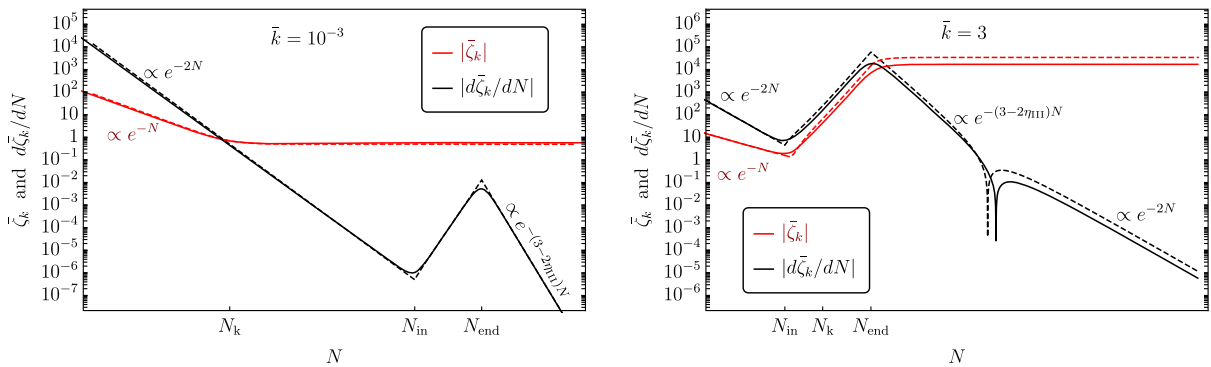


FIG. 13. Comparison of the time evolution of $|\bar{\zeta}_k|$ and $|d\bar{\zeta}_k/dN|$ computed numerically (solid lines) and with the analytical approximation (dashed lines) within the minimal dynamics presented in Sec. II B. We take $\bar{k} = 10^{-3}$ (left panel) and $\bar{k} = 1$ (right panel). To draw this figure we consider the benchmark values $\eta_{\text{II}} = 3.5$, $\eta_{\text{III}} = 0$, $\Delta N_{\text{USR}} = 2.5$ and $\delta N = 0.3$.

with $\epsilon(N)$ given by Eq. (32) for generic δN . In the limit $\delta N \rightarrow 0$ and at time $N = N_{\text{end}}$, we find

$$\begin{aligned} \lim_{\delta N \rightarrow 0} W(N_{\text{end}}) &= \frac{\bar{k}^3}{4} e^{(2\eta_{\text{II}}-3)(N_{\text{end}}-N_{\text{in}})} = \frac{\bar{k}^3}{4} \left(\frac{k_{\text{end}}}{k_{\text{in}}} \right)^{2\eta_{\text{II}}-3} \\ &= \frac{k^3}{4} \left(\frac{k_{\text{end}}^{2\eta_{\text{II}}-3}}{k_{\text{in}}^{2\eta_{\text{II}}}} \right). \end{aligned} \quad (\text{A12})$$

If we further take $\eta_{\text{II}} = 3$, then the above equation is compatible with Ref. [35].

We now consider the limit $\delta N \rightarrow 0$ and the case $\eta_{\text{II}} = 3$. In this case, it is possible to compute the function $\bar{\zeta}_q(N)$ by solving analytically the M-S equations in both the SR (for $N \leq N_{\text{in}}$) and USR (for $N_{\text{in}} \leq N \leq N_{\text{end}}$) regime and then matching the solutions at N_{in} , as done in Ref. [35] (see also Refs. [12,52]). We find ($x \equiv e^{\Delta N_{\text{USR}}}$)

$$\begin{aligned} |\bar{\zeta}_q(N_{\text{end}})|^2 &= \frac{x^6}{8\bar{q}^6} \left[9 + 18\bar{q}^2 + 9\bar{q}^4 + 2\bar{q}^6 + 3(-3 + 7\bar{q}^4) \cos\left(2\bar{q} - \frac{2\bar{q}}{x}\right) - 6\bar{q}(3 + 4\bar{q}^2 - \bar{q}^4) \sin\left(2\bar{q} - \frac{2\bar{q}}{x}\right) \right] \\ &\quad + \frac{x^5}{8\bar{q}^6} \left[12\bar{q}^2(-3 - 4\bar{q}^2 + \bar{q}^4) \cos\left(2\bar{q} - \frac{2\bar{q}}{x}\right) - 6\bar{q}(-3 + 7\bar{q}^4) \sin\left(2\bar{q} - \frac{2\bar{q}}{x}\right) \right] \\ &\quad + \frac{x^4}{8\bar{q}^6} \left[\bar{q}^2(9 + 18\bar{q}^2 + 9\bar{q}^4 + 2\bar{q}^6) + \bar{q}^2(9 - 21\bar{q}^4) \cos\left(2\bar{q} - \frac{2\bar{q}}{x}\right) - 6\bar{q}^3(-3 - 4\bar{q}^2 + \bar{q}^4) \sin\left(2\bar{q} - \frac{2\bar{q}}{x}\right) \right], \end{aligned} \quad (\text{A13})$$

which enters into the computation of Eq. (87).

-
- [1] S. Hawking, *Mon. Not. R. Astron. Soc.* **152**, 75 (1971).
 - [2] Y. B. Zel'dovich and I. D. Novikov, *Sov. Astron. AJ* (Engl. Transl.), **10**, 602 (1967).
 - [3] B. J. Carr and S. W. Hawking, *Mon. Not. R. Astron. Soc.* **168**, 399 (1974).
 - [4] P. Ivanov, *Phys. Rev. D* **57**, 7145 (1998).
 - [5] J. Garcia-Bellido, A. D. Linde, and D. Wands, *Phys. Rev. D* **54**, 6040 (1996).
 - [6] P. Ivanov, P. Naselsky, and I. Novikov, *Phys. Rev. D* **50**, 7173 (1994).
 - [7] M. Sasaki, T. Suyama, T. Tanaka, and S. Yokoyama, *Classical Quantum Gravity* **35**, 063001 (2018).
 - [8] A. Escrivà, F. Kuhnel, and Y. Tada, *arXiv:2211.05767*.
 - [9] O. Özsoy and G. Tasinato, *Universe* **9**, 203 (2023).
 - [10] B. Carr and F. Kuhnel, *Annu. Rev. Nucl. Part. Sci.* **70**, 355 (2020).
 - [11] A. M. Green and B. J. Kavanagh, *J. Phys. G* **48**, 043001 (2021).
 - [12] G. Ballesteros, J. Rey, M. Taoso, and A. Urbano, *J. Cosmol. Astropart. Phys.* **07** (2020) 025.
 - [13] N. Bhaumik and R. K. Jain, *Phys. Rev. D* **104**, 023531 (2021).
 - [14] K. Inomata, M. Kawasaki, K. Mukaida, Y. Tada, and T. T. Yanagida, *Phys. Rev. D* **95**, 123510 (2017).
 - [15] L. Iacconi, H. Assadullahi, M. Fasiello, and D. Wands, *J. Cosmol. Astropart. Phys.* **06** (2022) 007.
 - [16] S. Kawai and J. Kim, *Phys. Rev. D* **104**, 083545 (2021).
 - [17] N. Bhaumik and R. K. Jain, *J. Cosmol. Astropart. Phys.* **01** (2020) 037.
 - [18] D. Y. Cheong, S. M. Lee, and S. C. Park, *J. Cosmol. Astropart. Phys.* **01** (2021) 032.
 - [19] K. Inomata, M. Kawasaki, K. Mukaida, and T. T. Yanagida, *Phys. Rev. D* **97**, 043514 (2018).
 - [20] I. Dalianis, A. Kehagias, and G. Tringas, *J. Cosmol. Astropart. Phys.* **01** (2019) 037.
 - [21] K. Kannike, L. Marzola, M. Raidal, and H. Veermäe, *J. Cosmol. Astropart. Phys.* **09** (2017) 020.
 - [22] M. P. Hertzberg and M. Yamada, *Phys. Rev. D* **97**, 083509 (2018).
 - [23] G. Ballesteros and M. Taoso, *Phys. Rev. D* **97**, 023501 (2018).
 - [24] J. Garcia-Bellido and E. Ruiz Morales, *Phys. Dark Universe* **18**, 47 (2017).
 - [25] A. Karam, N. Koivunen, E. Tomberg, V. Vaskonen, and H. Veermäe, *J. Cosmol. Astropart. Phys.* **03** (2023) 013.
 - [26] S. Rasanen and E. Tomberg, *J. Cosmol. Astropart. Phys.* **01** (2019) 038.
 - [27] S. Balaji, J. Silk, and Y.-P. Wu, *J. Cosmol. Astropart. Phys.* **06** (2022) 008.
 - [28] J.-X. Zhao, X.-H. Liu, and N. Li, *Phys. Rev. D* **107**, 043515 (2023).
 - [29] D. Frolovsky and S. V. Ketov, *Universe* **9**, 294 (2023).
 - [30] K. Dimopoulos, *Phys. Lett. B* **775**, 262 (2017).
 - [31] C. Germani and T. Prokopec, *Phys. Dark Universe* **18**, 6 (2017).
 - [32] S. Choudhury and A. Mazumdar, *Phys. Lett. B* **733**, 270 (2014).
 - [33] H. V. Ragavendra and L. Sriramkumar, *Galaxies* **11**, 34 (2023).
 - [34] S.-L. Cheng, D.-S. Lee, and K.-W. Ng, *Phys. Lett. B* **827**, 136956 (2022).

- [35] J. Kristiano and J. Yokoyama, *Phys. Rev. Lett.* **132**, 221003 (2024).
- [36] A. Riotto, [arXiv:2301.00599](#).
- [37] J. Kristiano and J. Yokoyama, *Phys. Rev. D* **109**, 103541 (2024).
- [38] A. Riotto, [arXiv:2303.01727](#).
- [39] H. Firouzjahi, *J. Cosmol. Astropart. Phys.* **10** (2023) 006.
- [40] H. Firouzjahi and A. Riotto, *J. Cosmol. Astropart. Phys.* **02** (2024) 021.
- [41] S. Choudhury, M. R. Gangopadhyay, and M. Sami, [arXiv:2301.10000](#).
- [42] S. Choudhury, S. Panda, and M. Sami, *Phys. Lett. B* **845**, 138123 (2023).
- [43] S. Choudhury, S. Panda, and M. Sami, *J. Cosmol. Astropart. Phys.* **11** (2023) 066.
- [44] S. Choudhury, S. Panda, and M. Sami, *J. Cosmol. Astropart. Phys.* **08** (2023) 078.
- [45] J. M. Maldacena, *J. High Energy Phys.* **05** (2003) 013.
- [46] L. Senatore and M. Zaldarriaga, *J. High Energy Phys.* **12** (2010) 008.
- [47] E. Calzetta and B. L. Hu, *Phys. Rev. D* **35**, 495 (1987).
- [48] R. D. Jordan, *Phys. Rev. D* **33**, 444 (1986).
- [49] P. Adshead, R. Easther, and E. A. Lim, *Phys. Rev. D* **80**, 083521 (2009).
- [50] P. A. R. Ade *et al.* (BICEP/Keck Collaboration), *Phys. Rev. Lett.* **127**, 151301 (2021).
- [51] V. Assassi, D. Baumann, and D. Green, *J. High Energy Phys.* **02** (2013) 151.
- [52] C. T. Byrnes, P. S. Cole, and S. P. Patil, *J. Cosmol. Astropart. Phys.* **06** (2019) 028.
- [53] M. Taoso and A. Urbano, *J. Cosmol. Astropart. Phys.* **08** (2021) 016.
- [54] G. Franciolini and A. Urbano, *Phys. Rev. D* **106**, 123519 (2022).
- [55] M. Sasaki, *Prog. Theor. Phys.* **76**, 1036 (1986).
- [56] V. F. Mukhanov, *Sov. Phys. JETP* **67**, 1297 (1988).
- [57] M. S. Sloth, *Nucl. Phys. B* **775**, 78 (2007).
- [58] K. Inomata, M. Braglia, and X. Chen, *J. Cosmol. Astropart. Phys.* **04** (2023) 011.
- [59] P. R. Jarnhus and M. S. Sloth, *J. Cosmol. Astropart. Phys.* **02** (2008) 013.
- [60] P. Adshead, R. Easther, and E. A. Lim, *Phys. Rev. D* **79**, 063504 (2009).
- [61] S. Young, I. Musco, and C. T. Byrnes, *J. Cosmol. Astropart. Phys.* **11** (2019) 012.
- [62] V. De Luca, G. Franciolini, A. Kehagias, M. Peloso, A. Riotto, and C. Ünal, *J. Cosmol. Astropart. Phys.* **07** (2019) 048.
- [63] M. H. Namjoo, H. Firouzjahi, and M. Sasaki, *Europhys. Lett.* **101**, 39001 (2013).
- [64] X. Chen, H. Firouzjahi, E. Komatsu, M. H. Namjoo, and M. Sasaki, *J. Cosmol. Astropart. Phys.* **12** (2013) 039.
- [65] Y.-F. Cai, X. Chen, M. H. Namjoo, M. Sasaki, D.-G. Wang, and Z. Wang, *J. Cosmol. Astropart. Phys.* **05** (2018) 012.
- [66] S. Pi and M. Sasaki, *Phys. Rev. Lett.* **131**, 011002 (2023).
- [67] S. Passaglia, W. Hu, and H. Motohashi, *Phys. Rev. D* **99**, 043536 (2019).
- [68] D. G. Figueroa, S. Raatikainen, S. Rasanen, and E. Tomberg, *Phys. Rev. Lett.* **127**, 101302 (2021).
- [69] M. Biagetti, V. De Luca, G. Franciolini, A. Kehagias, and A. Riotto, *Phys. Lett. B* **820**, 136602 (2021).
- [70] D. G. Figueroa, S. Raatikainen, S. Rasanen, and E. Tomberg, *J. Cosmol. Astropart. Phys.* **05** (2022) 027.
- [71] E. Tomberg, *Phys. Rev. D* **108**, 043502 (2023).
- [72] V. Atal, J. Garriga, and A. Marcos-Caballero, *J. Cosmol. Astropart. Phys.* **09** (2019) 073.
- [73] G. Ferrante, G. Franciolini, A. Iovino, Junior., and A. Urbano, *Phys. Rev. D* **107**, 043520 (2023).
- [74] A. D. Gow, H. Assadullahi, J. H. P. Jackson, K. Koyama, V. Vennin, and D. Wands, *Europhys. Lett.* **142**, 49001 (2023).
- [75] G. Ferrante, G. Franciolini, A. J. Iovino, and A. Urbano, *J. Cosmol. Astropart. Phys.* **06** (2023) 057.
- [76] A. Iannicari, A. J. Iovino, A. Kehagias, D. Perrone, and A. Riotto, [arXiv:2402.11033](#).
- [77] A. M. Green, A. R. Liddle, K. A. Malik, and M. Sasaki, *Phys. Rev. D* **70**, 041502 (2004).
- [78] S. Young, C. T. Byrnes, and M. Sasaki, *J. Cosmol. Astropart. Phys.* **07** (2014) 045.
- [79] H. Motohashi and Y. Tada, *J. Cosmol. Astropart. Phys.* **08** (2023) 069.
- [80] S. M. Leach, A. R. Liddle, J. Martin, and D. J. Schwarz, *Phys. Rev. D* **66**, 023515 (2002).
- [81] G. L. Pimentel, L. Senatore, and M. Zaldarriaga, *J. High Energy Phys.* **07** (2012) 166.
- [82] O. Özsoy and G. Tasinato, *Phys. Rev. D* **105**, 023524 (2022).
- [83] S. Balaji, H. V. Ragavendra, S. K. Sethi, J. Silk, and L. Sriramkumar, *Phys. Rev. Lett.* **129**, 261301 (2022).
- [84] J. H. P. Jackson, H. Assadullahi, A. D. Gow, K. Koyama, V. Vennin, and D. Wands, *J. Cosmol. Astropart. Phys.* **05** (2024) 053.
- [85] G. Domènech, G. Vargas, and T. Vargas, *J. Cosmol. Astropart. Phys.* **03** (2024) 002.
- [86] E. Pajer, F. Schmidt, and M. Zaldarriaga, *Phys. Rev. D* **88**, 083502 (2013).
- [87] P. Creminelli and M. Zaldarriaga, *J. Cosmol. Astropart. Phys.* **10** (2004) 006.
- [88] Y. Akrami *et al.* (Planck Collaboration), *Astron. Astrophys.* **641**, A10 (2020).
- [89] D. J. Fixsen, E. S. Cheng, J. M. Gales, J. C. Mather, R. A. Shafer, and E. L. Wright, *Astrophys. J.* **473**, 576 (1996).
- [90] F. Bianchini and G. Fabbian, *Phys. Rev. D* **106**, 063527 (2022).
- [91] S. Bird, H. V. Peiris, M. Viel, and L. Verde, *Mon. Not. R. Astron. Soc.* **413**, 1717 (2011).
- [92] P. S. Cole, A. D. Gow, C. T. Byrnes, and S. P. Patil, *J. Cosmol. Astropart. Phys.* **08** (2023) 031.